DOTTORATO DI RICERCA IN

SCIENZE CLINICHE

-Ciclo XXVIII-

Coordinatore: Prof. Francesco Annunziato

"Sperimentazione in Vitro di un Sistema di Realtà Aumentata nella Chirurgia delle Neoformazioni Cerebrali"

Settore scientifico-disciplinare MED/27

Dottorando
Dott. Antonio Meola

Tutor
Chiar.mo Prof. Pietro A. Modesti

Coordinatore
Chiar.mo Prof. Francesco Annunziato

A.A. 2015/2016

A mio padre, per il coraggio di osare,

A mia madre, per il coraggio di riuscire.

.

Index

1. Synopsis

During the last 15 years, neuronavigation has become an essential neurosurgical tool when pursuing minimal invasiveness and maximal safety. Unfortunately, ergonomics of such devices are still not optimal. The neurosurgeon has to look away from the surgical field into a dedicated workstation screen. Then, the operator is required to transfer the information from the "virtual" environment of the navigation system to the real surgical field.

Augmented reality (AR) consists in overlapping a 2D or 3D, patient-specific, image-derived model of an anatomical detail (i.e. an organ) on a picture or video of the real surgical field. This process creates a new image, where reality and virtuality coexist, allowing an immediate transparent visualization of internal structures through superficial layers or the borders of surgical approaches. In this sense, the AR is the process of enrichment of reality with additional virtual contents. Thus, AR represents the next technological step of neuronavigation.

In neurosurgical oncology, there is a special need for AR to enhance the surgeon's perception of the surgical environment. The surgical field is often small and the neurosurgeon has to develop a "X-ray" view through the anatomical borders of the surgical approach itself in order to avoid unnecessary manipulation or inadvertent injuries to vascular or nervous structures.

With this aim in mind, we directed our efforts in two main directions: the informative content of AR guided neurosurgery, and the visualization tools of such information.

The first goal consisted in the understanding, integration and improvement of radiological techniques as a source of virtual information about tumor margins and the critical surrounding structures. In particular, we aimed to clarify the anatomy of several relevant white matter bundles both under physiological and pathological conditions, using the high-definition fiber tractography, as a complement to the traditional cranial CT and MRI. In the course of the study we also discovered a new white matter tract, the non-decussating dentatorubrothalamic tract, and we demonstrated that the superior fronto-occipital fasciculus does not exist.

The second goal consisted in improving the AR visualization tools. After a systematic review of the advantages and limitations of existing AR systems used in vivo, a novel AR system, based on a head mounted stereoscopic video see-through display (HMD), was used as an aid in complex neurological lesion targeting. For this purpose we created a newly designed patient-specific head mannequin featuring an anatomically realistic brain phantom with embedded synthetically created tumor and eloquent area. Two neurosurgeons in-training tested the clinical effectiveness of the AR system in a simulated high-risk neurosurgical scenario: the resection of a small tumor (or tumor portion) in the inferior frontal gyrus, while avoiding an adjacent eloquent area typically located in the posterior part of the same gyrus, namely the Broca's area. Conceptually, the exact location of the Broca's area can be extrapolated by the integration of the advanced radiological techniques, including the MRI and tractography.

From a surgical viewpoint, the optimal trajectory for accessing the lesion, as well as avoiding the eloquent area, was better defined by means of the AR guidance than without AR. Additionally, the presented AR system proved to be an effective aid in reducing the size of the skin incision and the craniotomy.

From a technical perspective, when compared to similar AR systems, the HMD-based AR neuronavigation herein presented, proved: to provide an unpreceded 3D visualization both of the surgical field and of the virtual objects, to provide an improved depth-perception of the augmented scene, to be ergonomic and unaffected by the parallax problem and to be very cost-effective. On the other hand, our mannequin itself might be used for training purposes, in combination or separately to the AR neuronavigator. Finally, the preliminary results herein presented strongly encourages to conducting a more structured study to prove its clinical effectiveness.

2. Introduction

2.1 From image guidance to Augmented Reality in Surgery

According to Medical Subject Headings, image guided surgery (IGS) includes all the surgical procedures performed with the aid of computers. The information presented can be a purely schematic, virtual representation of the actual surgical field details, or might integrate virtual contents with naive, non-processed information, at a various extent. So, mixed reality is defined as a continuum between the reality, a naive unmodeled environment, and virtuality, namely a completely modeled representation of reality.[1] Where an environment is located in such a continuum, corresponds to how much it is modeled rather then real.

Augmented reality (AR) is part of the reality-virtuality continuum: a virtual model of one or more environmental details is overlapped to the unmodeled reality.

In surgery, AR consists in overlapping a 2D or 3D, patient-specific, image-derived model of an anatomical detail (i.e. an organ) on a picture or video of the real surgical field. This creates a new image, where reality and virtuality coexist, allowing a transparent visualization of internal structures through superficial layers or the borders of surgical approaches.

Thus, the introduction of AR in the daily surgical armamentarium is expected to reduce the invasivity of surgical approaches, and consequently of blood loss and surgical time. On the other hand, a wider visualization of anatomical details reduces the risk of inadvertent injuries to critical structures, making the surgeon more confident when performing the procedures themselves.

Up to date, AR was applied to several surgical specialties including, but not limited to, orthopedics,[2] cardiac surgery,[3] urology,[4] general surgery.[5]

2.2 Image-guided Neurosurgery: new imaging techniques and new contents

The application of image-guidance to neurosurgery led the development of the so-called neuronavigation in the late 1980s.[6, 7] It rapidly became an important neurosurgical tool, mainly when attempting a tumor resection. The concept of neuronavigation is to guide an operation by using the preoperative images of the patient, primarily through tracking surgical tools and displaying their relative position to the patient by displaying virtual tools on the images. Thus, it has been widely used in neurosurgical procedures because it can help to reduce the invasiveness, improve the quality of the procedure, and shorten the operation time.

Neuronavigation is a multi-step process composed by: first, planning of the surgical strategy; second, registration, consisting in the process of recognition of the patient in the space by the neuronavigation systems equipped with an optical system; and finally navigation, namely the real-time display of the surgical planning during the actual surgical procedure.

The planning consists in the acquisition of patient specific images (i.e. MRI, CT, fMRI, tractography) by mean of a dedicated software. This allows manipulating and fusing different imaging modalities in order to identify surgical lesions, to create surgical trajectories into the brain, and eventually, to physically draw multiple areas to avoid. Ideed during brain tumor resections, the neurosurgeon invariably has to deal with several critical anatomical structures including arteries, veins, nerves as well as “eloquent” areas. These are, by definition, cortical or subcortical areas, whose resection (or a inadvertent injury) likely causes neurological deficits.

Thus, from a neurosurgical view point, every reasonable effort has to be done in two main directions: the informative content of image-guided neurosurgery, and the visualization tools of such information.[8]

The first goal consists in the understanding, integration and improvement of radiological techniques in order to obtain a detailed representation of the lesion margins and of the critical surrounding structures.

The second goal can be achieved by improving the technological tools that allows the neurosurgeon to visualize the surgical plan more efficiently.

Thus, we provide a synthetic review of the most advanced techniques of brain imaging that, along with the traditional techniques (CT, MRI and angiography), are expected to expand the informative content of neuronavigation and AR. These techniques include: tractography, magnetoencephalography (MEG), repetitive transcranial magnetic stimulation (rTMS) and functional magnetic resonance imaging (fMRI). In fact, each of these techniques might be used to reconstruct 3D models of relevant anatomical or functional structures.

Tractography

The application of magnetic field gradients allows sensitizing MR imaging to the random, thermally driven motion (diffusion) of water in the direction of a determined field gradient. By definition, diffusion is directionally dependent, namely anisotropic, in white matter bundles, as axonal c cell membranes represent barriers to water motion in directions different respect to their own orientation.[9, 10] Thus, the direction of maximum diffusivity represents the white matter bundle orientation. This information is represented by the diffusion tensor, a mathematic model of diffusion in three-dimensional space. The tensor allows evaluating the diffusivity of the water molecules in any direction and, more importantly, in the direction of maximum diffusivity. Thus, the direction of maximum diffusivity may be visually represented by using red, green, and blue (RGB) color coding, resulting in a easy-to-understand map of local fiber direction in each part of the brain. From such a map, a three dimensional reconstruction of white matter bundles can be derived by the application of a proper algorithm. This process is known as tractography.[11]

Anyway, current tractographic algorithms has a limited ability to resolve fiber tract terminations near cortical surfaces (the termination problem) and to follow the direction of different tracts when they cross each other (the crossing problem), potentially resulting in artifacts, false tracts and false continuations.[12, 13] In an attempt to resolve these limitations new advanced fiber tractography methods were applied to a template of 488 subjects from the Human Connectome Project (Q1-Q3 release, WU-Minn HCP consortium) (HCP-488).

The WU-Minn HCP consortium is an ongoing project led by Washington University, University of Minnesota and Oxford University, which aims to define in detail a "map" of human brain connectivity and function. It will allow analyzing and comparing brain circuits, behavioral features, and genetic tracts within the same subject and between subjects.[14] The reconstructed data of the 488 subjects of the Q1-Q3 release, were averaged to create a representative template (DSI studio, freely downloadable at: http://dsi-studio.labsolver.org/download-images). Whole brain fiber tracking was conducted using an advanced deterministic fiber tracking algorithm.[15] The resulting fiber tractography method is known as high-definition fiber tractography (HDFT).

The application of such a method allowed clarifying misunderstood anatomical details of the human brain connections. As an example the superior fronto-occipital fasciculus (SFOF) was regarded as a bundle connecting the frontobasal cortex to the parieto-occipital cortex,[11] and its assumed role was visuospatial processing.[16] The application of the proposed tractography algorithm allowed discovering that this bundle does not exist (Figure 2):[17] the image presented by previous tractographic studies[9-11, 18, 19] was affected by two false continuations, namely between the superior thalamic peduncle (STP) with the stria terminalis (ST) and between the ST and the posterior thalamic peduncle (PTP). Our data are in full agreement both with the results of our microsurgical cadaveric dissection and with previous histological analysis.[20]

The HDFT was also used to reveal the existence of unknown brain connections. Traditionally, the cerebellar hemisphere is known to elicit only ipsilateral motor influence. In fact, the main cerebellar output, namely the dentatorubrothalamic tract (DRTT) is classically described as a bundle arising from the deep cerebellar nuclei, mainly the dentate nucleus (DN), running in the superior cerebellar peduncle (SCP), and then completely decussating to the contralateral red nucleus (RN), to ascend to the thalamus and finally to the cortex.[21] Thus, motor deficits related to unilateral hemispheric cerebellar lesions, such as strokes, hemorrhages, and tumors, would be expected to influence only the ipsilateral limbs.[22]

Surprisingly, the cerebellar hemisphere clearly influences bilateral limb movements, as demonstrated by human fMRI studies,[23, 24] human rTMS studies,[25, 26] human motor performance studies,[27-29] as well as neurophysiological studies,[30, 31] and experimental lesional studies in monkey.[32, 33]

We found that the connections of the DN with the RN and thalamus are bilateral and not only contralateral, as traditionally accepted.[34] We identified the "classical" decussating DRTT fibers and an

ipsilateral non-decussating path that is the nd-DRTT (Figure 3). Within each of those 2 tracts some fibers stop at the level of RN, forming respectively the dentatorubrothalamic tract (DRT) and the non-decussating dentatorubrothalamic tract (nd-DRT).

These results offer a potential anatomical explanation for bilateral limb motor effects of cerebellar hemispheres under physiological conditions, and for bilateral limb motor impairment in pathological situations.

In a similar fashion HDFT can be used to depict anatomical connections in brain malformations.

As an example, we reported a case of a 60-year-old-man referring worsening headaches and electrical shooting sensation in the nuchal region. Neurological examination revealed slurred speech, sudden, repetitive, non-voluntary head movements, imbalance and gait impairment with difficulty to stop walking forward. Childhood development of upright walking was delayed to age 6. Psychological examination revealed a high-functioning individual with IQ of 70. The MRI scan showed an almost complete cerebellar agenesis with a minimal residual upper vermis and a hypoplastic brainstem (Figure 3A). The MRI diffusion tensor imaging analysis in normal subjects (Figure 3B) revealed, from medial-to-lateral, the superior, inferior and middle cerebellar peduncles. Unexpectedly, although the cerebellum is almost undetectable, the cerebellar peduncles are still present, although remarkably atrophic, and the spatial relationships between them are preserved.[35]

The HDFT was applied to the definition of normal anatomy of the white matter bundles of the brainstem, as well as in the presurgical planning of brainstem lesions. Brainstem surgery requires not only precise understanding of safe entry zones but also detailed knowledge of the narrow surgical corridors and course of brainstem white matter bundles. Up to date, only a few DTI-based studies of brainstem connections exist.[36-43] Compared with the state-of-the-art diffusion MRI acquisition, the previous studies had relatively low spatial resolution, and failed to identify several major fiber pathways. These studies have used DTI in as the method. DTI-based techniques, however, are unable to solve accurately the crossing of fibers and to identify accurately the origin and termination of fibers, potentially resulting in artifacts and false tracts. These limitations, well known in the supratentorial space, are even more remarkable when dealing with the crowded tracts of the brainstem. In addition, the number of subjects enrolled in previous studies is very small (up to 10), which limits considerably any general conclusion about brainstem fiber tract

anatomy. We applied HDFT to the HCP-488 in order to describe the brainstem pathways, and validated our findings with histological analysis that still represents the gold standard for anatomical validation. The pathways included the cerebellar peduncles, the corticospinal tract (CST), the corticopontine tracts (CPTs), the medial lemniscus (ML), the lateral lemniscus (LL), the spinothalamic tract (STT), the rubrospinal tract (RST), the central tegmental tract (CTT), the medial longitudinal fasciculus (MLF), and the dorsal longitudinal fasciculus (DLF). Then, the reconstructed 3-dimensional brainstem structure (Figure 5) was sectioned at the level of classical surgical approaches, namely: supracollicular, infracollicular (Figure 6), lateral mesencephalic sulcus, perioculomotor, paratrigeminal, anterolateral approach to the medulla, and retro-olivary sulcus approach. Finally, the advanced knowledge on normal brainstem connections, was applied to identify the displaced or disrupted tracts surrounding lesions in this area. This approach provided for the first time to reconsider the safe entry zones as described in classical anatomy, under the light of a high resolution patient-specific map of the brainstem connections (Figure 7).

Magnetoencephalography (MEG)

MEG refers to an imaging technique of direct registration of magnetic fields produced by the human brain. This method has several advantages over some other brain mapping methods. In fact, electroencephalography (EEG) and electrocorticography (EcoG), respectively the non-invasive and the invasive method for brain electrical activity registration, are affected by signal distortion due to several interfaces that the electrical signal goes through. Conversely, MEG registers magnetic fields that, by their nature itself, are not subject to distortion. Additionally, the MEG has an unpaired temporal resolution respect to fMRI. In fact, fMRI registers regional brain changes of oxygenated blood, meaning that there is latency of few seconds between the neural activation and the detectable vascular coupling. Conversely, MEG is a direct registration of neural activity. Its temporal accuracy is about 1 ms, while its spatial accuracy is 0,1-1 cm, making this technique a good candidate for neurosurgical applications.[44]
From a clinical viewpoint, MEG was used in patients affected by brain tumors, aiming to map the sensorimotor cortex,[45, 46] auditory cortex[44, 47] and visual cortex.[48]

Repetitive transcranial magnetic stimulation (rTMS)

rTMS is a noninvasive technique that creates a precise, local magnetic field that induces an action potential in a well delimited population of neurons. Thus, the patient's MRI data can be coregistered with the TMS software, allowing for precise delivery of the magnetic field to the cortical surface. On the basis of a patient specific MRI-map, a magnetic field is delivered to specific regions of functional cortical areas, resulting in underneath neuron activation. Recent data indicate that TMS-based motor maps correlate well with DCS in the operating room.[49] TMS has also used as preoperative test for localization of language functions, even if results are less consistent compared to motor mapping. TMS represents a very promising tool not only for preoperative mapping of various cerebral functions but also to induce cortical plasticity before and after tumor resection.[50]

Functional magnetic resonance imaging (fMRI)

fMRI is a non-invasive imaging technique, based on the theoretical principle that neuron activity can be indirectly monitored by assessing the induced blood flow. More precisely, the fMRI measures regional brain concentration of deoxyhemoglobin that in this case can be fully assimilated to an endogenous contrast agent. The signal derived from deoxyhemoglobin concentration is also known as blood oxygenation level dependent (BOLT) signal.

Although several applications were proposed for fMRI in medicine, the role of fMRI is mainly dedicated to the mapping of brain eloquent areas. In fact, the execution of proper tasks (such as motor or language tasks) elicits regional changes in blood flow, detected by fMRI.[51] Although very promising, fMRI is subject to a number of artifacts and mandates a solid experience in imaging processing. In fact, nowadays the gold standard for brain mapping is the intraoperative direct cortical electrical stimulation.

2.3 Augmented Reality in Neurosurgery: a systematic review

During the last 15 years, neuronavigation has become an essential neurosurgical tool for pursuing minimal invasiveness and maximal safety.[7] Unfortunately, ergonomics of such devices are still not optimal.[6] The neurosurgeon has to look away from the surgical field into a dedicated workstation screen. Then, the operator is required to transfer the information from the "virtual" environment of the navigation system to the real surgical field. The virtual environment includes virtual surgical instruments and patient-specific virtual anatomy details (generally obtained from pre-operative 3D images). AR allows merging data from the real environment with virtual information and vice-versa.[52] In the context of surgical navigation, AR may represents the next significant technological development because AR complements and integrates the concepts of traditional surgical navigation that rely solely on virtual reality.[53] The main goal of AR systems is to provide a real-time updated 3D virtual model of anatomical details, overlaid on the real surgical field. In this sense, the AR reality is the process of enrichment of reality with additional virtual contents.

In neurosurgery, there is a special need for AR to enhance the surgeon's perception of the surgical environment. The surgical field is often small and the neurosurgeon has to develop a "X-ray" view through the anatomical borders of the surgical approach itself[54] in order to avoid unnecessary manipulation or inadvertent injuries to vascular or nervous structures, which becomes even more important with the introduction of minimally invasive neurosurgery mandating the smallest possible accesses for a given intracranial pathology.[55] Although the benefits to patients of minimally invasive neurosurgery are well established, the use of small approaches still represents a surgical challenge. Although AR in neurosurgery is a promising frontier, and several devices have been tested in vitro,[8, 56] the clinical experience with such systems appears to be quite limited.[6, 7, 57-66] We present a literature review aiming to: describe and evaluate the advantages and shortcomings of each of the different AR setups tested in vivo in humans; to understand the efficacy of AR in the treatment of neurosurgical diseases; and, to define potential future research directions.

2.3.1 Methods

The present review was conducted according to the PRISMA statement criteria.[67] The literature search was updated to September 30th, 2015. No other temporal limits were applied. The search was restricted to human studies. Inclusion criterion was: report of a human in vivo application of AR in any neurosurgical procedure. Exclusion criteria were: surgical simulation in virtual environment, in vitro studies, language of publication other than English, lack of new original experiments on humans, field of application other than neurosurgery, commentaries, and abstracts. The search was performed using the PubMed database and scanning reference lists of the resulting articles. The search terms were "Augmented reality" and "Neurosurgery". Eligibility assessment was performed independently in an unblinded standardized manner by two reviewers (AM and FCa). Disagreements between reviewers were resolved by consensus. The following clinical data were extracted from each paper: neurosurgical subspecialty of application (neurovascular surgery, neuro-oncological surgery, non neurovascular, non-neuro-oncological), lesion pathology, and lesion location. We evaluated a number of additional relevant technical aspects, as listed, in part, in the Data, Visualization processing and View (DVV) taxonomy published in 2010:[56] real-data source, virtual-data source, tracking modality, registration technique, visualization processing (AR visualization modality), display type where the final image is presented, the perception location (where the operator focused).

Unfortunately, qualitative parameters concerning the clinical usefulness and feasibility of the presented systems were not gathered primarily because of the subjective nature of the evaluation by the operators and the lack of consensus as to the definition of the qualitative parameters and consequently, the evaluation tools, such as questionnaires. In a similar fashion, the accuracy of the AR systems was not included because, when reported, its definition was not consistent across different papers, obviating a meaningful comparison .

Finally, due to the nature of the studies (small case series) and the subjective nature of the qualitative assessments, publication bias should be considered. For the same reasons, no statistical analysis was performed.

2.3.2 Results

A total of 18 studies were included in our review. The PubMed search provided 60 items. No duplicates were identified. Of these, 44 studies were discarded because they did not meet the inclusion criteria: four papers were written in languages other than English, seven were in vitro studies, five were virtual reality studies, nine were reviews or commentaries, 12 papers were about disciplines other than neurosurgery (i.e., maxillofacial surgery, ENT surgery), seven papers were not pertinent to AR. The full text of the remaining 16 citations was obtained. After carefully reviewing the bibliography of each of the papers, two additional citations were included. No other relevant unpublished studies nor congress abstracts were included. To the best of authors' knowledge, no other pertinent papers are available today.

Table 1 summarizes the 18 papers published from 1996 to September, 2015. The specific technical advantages and shortcomings of each system in the clinical setting are discussed below in section 4.1; the clinical applications of AR in neurosurgery are illustrated in section 4.2 and Table 2.

Six of the 18 studies reported neuro-oncological applications only (one of them mainly reported epileptogenic tumors)[68], six reported neurovascular applications only, five reported both neuro-oncological and neurovascular applications , and one reported a neuro-oncological, neurovascular, non-neuro-oncological non neurovascular application, the use of AR for external ventricular drainage placement.[60]

The lesions listed in Table 2 are classified by pathology type. A total of 195 treated lesions were analyzed in the selected works. Of these, 75 (38.46%) were neoplastic lesions, mainly gliomas (14 lesions, 7.17%) and meningiomas in supratentorial (12 lesions, 6.15%) or infratentorial/skull base (7 lesions, 3.58%) locations, pituitary adenomas (12 lesions, 6.15%) and metastases (11 lesions, 5.64%). There were 77 (39.48%) neurovascular lesions, mainly aneurysms of the anterior circulation (39 lesions, 20% of the total), and posterior circulation (four lesions, 2.05% of the total), cavernomas (20 lesions, 10.25%), AVMs (eight lesions, 4.10%). Non neoplastic, non vascular lesions included just one case (0.51% of total) of external ventricular drainage under AR guidance. The histology was not specified for 42 lesions (21.53%).

The “epileptogenic lesions” (40 lesions, 20.51%) were reported to be mainly tumors. Adding these lesions to the neoplastic lesions listed above (75), we may conclude that the neuro-oncological application is the most frequent type of use for AR in neurosurgery.

The Virtual-reality sources were: CT (13 studies), angio-CT (four studies), MRI (14 studies), angio RM (seven studies), functional MRI (one study), tractography (one study), and angiography (one study). The real-data sources were the microscope (eight studies), different types of cameras (four studies in total), including hand-held cameras (four studies) and head-held cameras (two studies), direct patient view with or without the interposition of a semitransparent mirror (one study each), endoscope (one study), X-Ray fluoroscopy (one study) and finally, a rudimentary head-mounted display (one study). Tracking was not needed in four setups, for, as performed, optical trackers were generally used (13 studies). Magnetic tracking was reported as used in only one of the oldest reports in 1996.[68] Patient registration was mainly based on superficial fiducial markers (six studies), on face surface matching systems (six studies), or on manual procedures/refinement (five studies). Skull-implanted or dental-fixed fiducials were used in two older reports in 1999 and 2004.[58, 59] Visualization processing allowed for the representation of virtual reality in several different ways including: surface mash (eight studies), texture maps (four studies), wireframes (three studies) and transparencies (three studies). Older reports described rudimentary visualizations: in one case,[68] the MRI slices were directly visualized in a fashion similar to the current neuronavigation devices; in another case,[64] a light field object rendering was performed. The display type determines the perception location that can be a remote monitor (eight studies) or the patient himself (10 studies). The latter perception location is achieved by using several different displays, including microscope eyepieces (five studies) or oculars via an external beam (two studies), tablet display, light field display with a 45 degree-oriented mirror, or an image created by a common video-projector (one study each).

2.3.3 Discussion

AR in Neurosurgery: technical implementations.

AR systems are composed of functionalities and devices that may be the same although used in different implementations. The real and virtual data source, its registration with the real content, the visualization of the AR content, and all the other factors shown in Table 1 are often performed with similar or exactly the same approach in different systems as described in the reported papers. Therefore, the discussion of some parts of selected papers reported here may appear somewhat redundant. We describe the papers grouping them by function of the real-data source as the type of capturing device used during the actual procedure is, from a surgical point of view, most important.

In most of the systems, the real data source is a surgical microscope. These systems allow overlaying 3D projections derived from preoperative surgical images into bilateral eyepieces of the binocular optics of the operating microscope, precisely aligned with the surgical field.[58, 59, 62, 63, 66, 69-71] To achieve a coherent fusion between real images and virtual content, these systems monitor microscope optics pose, focus, zoom, and all internal camera parameters.[72] This is an important advantage as other, simpler, systems require manual alignment with the surgical field.[60] The microscope based AR system represented by MAGI (microscope-assisted guided interventions), requires an invasive preoperative placement of skull-fixed fiducials and/or locking acrylic dental stents. More recently, surface based registration approaches have been used[62] without any additional referencing device as traditional modern neuronavigation systems.

It is significant that a microscope based AR system does not require the bayonet pointer typical of the common neuronavigation systems. In traditional neuronavigation systems, the bayonet pointer, tracked and shown in the external display, is the sole link between the real and the virtual environment. In fact, in order to see the correspondence between a real and a virtual point, the surgeon places the pointer tip on a

real anatomical target and observes its correspondence with the virtual one. In an AR scene, the correspondence between the real and virtual worlds is shown on the augmented images themselves without any additional physical device as a pointer, which might be a potential source of damage in the surgical field. Additionally, when brain shift occurs during intradural maneuvers, the AR view can be used as a guide for a limited correction of the initial image coregistration.[70, 73]

A special type of microscope based AR system is created by a neuronavigation-tracked microscope that serves uniquely as an input source for software integrating the data with preoperative virtual models.[71] The image is not displayed in the microscope, but rather, on a screen separate from the actual surgical scene. This is probably due to technical issues related to the re-send of the augmented images as input data to the microscope display. These microscope based AR systems have two main shortcomings: first, the microscope itself is not practical for the initial macroscopic part of the surgical procedure, consisting of skin incision, craniotomy, and dural opening; second, current microscopes display only a monoscopic visualization of the surgical field.[6] As a consequence, a potential stereoscopic virtual image is superposed on a bidimensional field. From a practical point of view, there are perceptual issues particularly related to depth perception of an AR scene.[6]

In four papers, the real data source was an additional hand-held and/or head-held camera.[6, 7, 60, 74] These systems are based on the use of a camera connected to a neuronavigation system. Currently, four main set-ups have been reported.

The Dex-Ray[6, 74] consists of a small, lipstick-shaped video-camera positioned on a tracked handheld pointer. The AR scene consists of the virtual rendering of a 3D dimensional virtual model superimposed on a bidimensional (monoscopic) view of the surgical field. Finally, the scene is shown on a display remote from the patient. Dex-Ray has several advantages and some limitations. There is a perfect alignment between the pointer and the camera so the surgeon is aware of the spatial relationship between the tip of the pointer, the borders of the surgical corridor, and the target. Nevertheless, this feature has two limitations: first, in deep and narrow corridors, the camera has a limited ability to depict the anatomical structures due to lack of light and unsatisfactory magnification. Second, the surgeon's viewpoint is different from that of the camera resulting in two main consequences: first, oculomotor issues occur due to

camera movement, and second, the different point-of-view raises uncertainty as to the actual position of camera-recorded objects (parallax problem).

Additionally, the Dex-Ray requires the surgeon to look away from the surgical field to a screen where the AR scene is shown, rendering this setup quite similar to common neuronavigation systems. Unlike the microscope, the Dex-Ray can be handled easily without obstruction of the surgical field, and can be conveniently used in all steps of the surgery, from skin incision to tumor resection.

The second camera based set-up is a quite similar one. The AR created overlapping intraoperative pictures (taken using a standard digital camera) on a 3D virtual model of the brain.[60] The virtual model was elaborated by dedicated neuroimaging 3D rendering software. The "real" intraoperative picture and the virtual model were matched using anatomical landmarks --sulci and gyri -- and shown to the surgeon with a bit of delay. The AR system was then validated by verifying the actual position of the surgical target with intraoperative US or stereotactic biopsy. The main advantage of this system is that it is extremely cost-effective, making it a suitable option in developing countries where traditional commercially available neuronavigation systems are not available.[60] The two main disadvantages are that the image-guidance is not displayed in real-time so the delay depends on the frequency of acquired pictures and that the guidance becomes unreliable when lesions are far from the cortical surface because the sole anatomical landmark is almost lost. Conversely, it works surprisingly well for lesions hidden in the depth of a sulcus.

Recently, a new system was designed by using a hand-held or head-held camera tracked by a classical neuronavigation system.[7] The AR scene was displayed on a separate monitor by overlapping the 3D virtual model, as acquired by the camera, onto the real bidimensional surgical field.. The head mounted camera partially resolves the issues related to a conflicting point of view for at least camera movement. Nevertheless, it still requires that the surgeon look away from the actual surgical scene to observe the AR scene on a separate screen. Additionally, the point of view of the camera is not aligned with surgeon's line of sight. Consequently, the eye-hand coordination may constitute a challenge.

More recently, a tablet based-AR system[65] was applied to neurosurgery. It consists of a navigational tablet that superimposes a virtual 3D model on the surgical field as it is recorded by the tablet's posterior camera. In this case, the camera's point of view can be considered aligned with the surgeon's line of sight,

offering favorable ergonomics in terms of eye-hand coordination. However, the tablet cannot be draped so a second surgeon needs to hold the tablet while the operator performs the surgery. Although the tablet allows magnification of the surgical field, it cannot provide the magnification and resolution necessary for microsurgical use.

The real-data source can be represented by the direct view of the patient's head. Two systems were proposed with this aim in mind. One is based on commercially available video projectors with LED technology.[75] The virtual image is projected onto the patient's head and it is rigidly and statically manually registered by moving the head or the projector up to align fiducial points. The main advantage is a potential intuitive visualization of the site of the skin incision and craniotomy (not explained by the authors) with a highly ergonomic setup, potentially resolving the eye-hand coordination problem. Unfortunately, the point-of-view of the operator is not the same as that of the projector, so that a parallax error is created, primarily for deep structures.

In 1997, a new, interesting AR system was created,[64] with a paradigm completely different from the previously described systems. It has continuously been improved during the ensuing years until the present. [76, 77] It consists of a semi-transparent mirror positioned at 45° in front of a light field display[78] developed with the integral imaging approach.[79] The display technology is the same as that employed in glass-free 3D television and allows obtaining a realistic full-parallax view of a virtual scene. The user can perceive motion parallax moving in respect to the display. The half mirror allows the user to see the patient's head with his/her unaided eyes and it is mixed with the full parallax light field rendering of the virtual information. The registration of the CT or MRI patient specific 3D model with the patient's head is manually performed aligning artificial markers.[80] The main advantage of the system is the full parallax visualization of the virtual information and the unaided view of real surgical environment, an advantage in a camera mediated view in cases of open surgery.

The application of the AR to endovascular surgery consisted of the superimposition of a CT or MRI-derived 3D model of the vascular tree and its lesions on the real bidimensional image acquired, in this case, with angiography.[61] Since the craniotomy is not needed, the brain shift is null in this application field. Accordingly, it can be considered the one AR system that is completely reliable for surgical access into the brain.

The use of an endoscope with AR consists of the superimposition of virtual 3D models, obtained, as in the previous case, from CT or MRI images on the bidimensional view of the surgical field as acquired by the endoscopic camera.[57] It requires registration of the patient's head and the tracking of the rigid endoscope itself. Two types of information were shown on the traditional endoscopic monitor: the surgical target (and surrounding critical structures), and the position of the endoscope inside the nasal cavities. The second aspect may be especially important when an angled endoscope is used as the endoscope axis is different from the surgeon's view of the axis. Typical limitations of common endoscopes still persist, including the bidimensional view of the operative field and a limited magnification ability in respect to the surgical microscope.

The oldest system reported in our review in 1996, did not show the virtual information superimposed and aligned with the real anatomy.[68] The graphic user interface essentially shows the surgeon the tip of a magnetic tracked digitizer in respect to the CT or MRI pre-operative images as in traditional (non-AR) neuronavigators. The system, a pioneer, can be considered a first example of AR as the authors employed a semi-transparent head mounted display so as to offer the user the possibility of seeing the navigator images and the real patient at the same time.

AR in Neurosurgery: clinical applications

AR has been applied to a wide range of diseases, including neoplastic, vascular, and other lesions (non-neoplastic non-vascular) as shown in Table 2. Nevertheless, the small number of cases in each series allowed only a qualitative assessment of the usefulness of AR in such neurosurgical procedures.

In neuro-oncological surgery, the AR has been applied in open treatment, mainly of gliomas and meningiomas. The largest tumor series[6, 59] reports an advantage in minimizing skin incisions and craniotomies. When the dura is to be opened, the AR allows a clear visualization of the venous sinuses underneath: for example, in the case of falcine meningiomas,[6, 74] the sagittal sinus can be seen as a virtual model, and spared. In addition, when tumors are hidden in the depths of a cerebral sulcus, the visualization of the tumor shape under the brain surface can aid in the selection of the sulcus to be dissected.[60] When the surgeon performs the corticectomy and tumor resection, the relevant surrounding

vascular and nervous structures can be visualized, including eloquent areas and white matter tracts.[7] In an older, yet broad series of mixed oncological and epilepsy cases, AR allowed reducing craniotomy size needed to position subdural electrodes monitoring cortical activity.[68] In skull base surgery, the AR provides an optimal visualization of cranial nerves and major vessels and their relationships with bony structures,[59] potentially reducing morbidity and mortality. This advantage is especially relevant in endoscopic endonasal approaches. In fact, AR allows the surgeon to orient his tracked instruments in the nasal cavities perfectly, having a precise awareness of the midline position and, when the approach moves laterally, visualizing the carotids and optic nerves.[57] Such an advantage is particularly relevant when the endonasal anatomy is distorted by previous interventions.

In vascular neurosurgery, the AR was mainly applied to the open treatment of aneurysms[63, 66] and AVMs,[62] and to the endovascular treatment of aneurysms.[61]

The microscope based AR systems were found to be a particularly useful asset in neurovascular surgery because they improve the craniotomy placement and dural opening[62, 63, 66] as also demonstrated in neuro-oncological cases.[58, 59] Specifically, microscope based AR systems were useful in aneurysm treatment because they allowed optimal adjustment of the head position, minimizing subarachnoid dissection, and selecting the proper clip placement by a thorough visualization of the vascular anatomy near the aneurysm itself.[63] Furthermore, when by-pass surgery was the selected treatment option for multiple aneurysms, the microscope based AR systems allowed for a reliable identification of the donor vessel and of the recipient intracranial vessel.[66] In the case of AVMs, results were less encouraging. In fact, microscope-based AR systems allowed a reliable visualization of the main arterious feeders of an AVM, indicating precisely where proximal control should be performed in case of an intraoperative AVM rupture. However, microscope-based systems were not able to reveal the detailed anatomy of vessels surrounding or actually feeding the AVM, a detail of critical importance during AVM resection. The information about AVM venous drainage seems to be irrelevant because a large number of cases underwent preoperative embolization.

Microscope-based AR systems were found to be a useful tool for resecting cavernomas close to eloquent areas or deeply-seated.[69] Unfortunately, the virtual component may partially obstruct the surgeon's point of view and not function when the cavernoma itself has been reached surgically.

AR also dramatically improved the endovascular treatment of cerebral aneurysms. In fact, the angiographic visualization of cerebral vessels does not allow the observer any intuitive deduction about the spatial relationship between structures. A 3D model of one or more vascular branches is a valuable aid for the surgeon.[61]

Finally, AR can also improve the treatment of non-neoplastic non-vascular pathology, as in the case of hydrocephalus secondary to subarachnoid hemorrhage.[60] The external ventricular drain positioning can be easier and faster, especially if the lateral ventricle is not well dilated yet due to sudden obstruction of the ventricular system.

AR in neurosurgery: between few certainties and many open problems

AR in neurosurgery was demonstrated as a useful asset in different subspecialties. There is a wide consensus that the optical tracking was the best option for AR systems in neurosurgery,[81] being used in 13 out of the 18 studies. In fact, optical tracking is very practical because does not require wires to connect the tracked object. Additionally, it is promptly available because it can rely on widely available cameras included in smartphones, tablets,[65] digital recording cameras.[7] The main shortcoming is that tracked objects have to be in line of sight of the tracking system. In a similar fashion, in largest part of the reported studies the image registration is based on fiducial markers or on skin surface identification. These two techniques demonstrated to be faster and more accurate respect to the manual registration.[82]

On the other hand there are a number of uncertainties limiting the introduction of AR in the daily practice. Currently, there are no prospective studies showing a significant difference between AR-aided surgeries versus navigation guided procedures in terms of morbidity, mortality, and clinical effectiveness. Further, the monetary cost of the different systems has not yet been determined. The necessary equipment for microscope based AR systems is primarily based on a neuronavigation system and a surgical microscope that are available in most modern operating rooms and their introduction into daily practice would not require additional costs. Some AR systems may also be cheaper than a standard neuronavigation system. In fact, in developing countries, very rudimentary AR systems, composed of a 3D rendering software

running on a computer and a digital camera[60] have partially replaced the use of neuronavigation systems, although with evident limitations.

From the technical point of view, there are several limitations. The depth perception of the overlaid 3D models is still quite difficult for all the AR systems.[83, 84] Binocular cues, partially offered by 3D stereoscopic displays, are not always sufficient for inferring the spatial relationships between objects in a three-dimensional scene. For this reason, many researchers try to improve depth perception by means of visualization processing techniques.[56] For example, specific color-coding, one of several methods, can be associated with the distance from the surgical target.[57] Other more sophisticated tools consist of progressive transparency of colors as the structures are deeper.[85]

The visualization processing is a broad topic that is relevant beyond depth perception itself. It affects the global manner ("style") that is used to represent the virtual content. From a practical point of view, visualization processing should be as simple and intuitive as possible, resembling the real-life experience: wireframes and texture maps are less intuitive than surface meshes because the latter realistically clearly represent the margin and shape of the object of interest. Indeed, they were used in seven of the more recent studies (Table 1).

The crowding of the surgical view is an additional issue. The virtual models should be presented to the surgeon, observing a principle of maximal effectiveness of the information. Only essential virtual details should be presented because the overlapped models may hide a part of the actual surgical field. This issue could be a potential source of morbidity and mortality. Similarly, all AR systems that require the surgeon to look away from the surgical field eliminate this risk.

An additional crucial aspect is the different points-of-view of the same surgical target that can be achieved by the surgeon's eye and optic devices (the parallax problem). When the surgeon's point-of-view is the same as that of the real-data source, there is no mismatch between what the operator sees and what the device actually captures. Conversely, when the operator and the data-source have different points-of-view, there may be uncertainty as to the actual position of the target.[6] The position of the AR display in relation to the surgeon is very important for future developments. Conceptually, when the AR is displayed on an external monitor,[6, 60, 71, 74] the surgeon has to move his/her attention from the actual surgical field to the monitor in order to gather information that will be "mentally" transferred to the real surgical field, as

currently occurs with the neuronavigation systems. In contrast, perception localization on the patient is much more intuitive. The goal can be achieved both by the unaided eye,[75] or by devices presenting the AR scene in the line of view between the surgeon and the surgical field, as in the case of the microscope,[62, 63, 66, 69, 70] the tablet,[65] and the light field display.[64]

The adequacy of an AR system should also be evaluated in respect to the different procedures or steps in the procedure. When only a macroscopic view of the surgical field is required (i.e., ventricular drain placement, standard craniotomy), microscope-based AR systems are potentially impractical because of the ergonomics of the microscope itself. When a relevant magnification is required, the microscope-based AR systems appear to be the best option.

Great effort should be invested in not only improving the visualization of 3D models, but also in introducing information derived from new advanced imaging techniques. AR systems represent a suitable option for multimodal imaging integration involving not only CT, MRI (and related techniques), and angiography, but also other techniques such as magnetoencephalography and transcranial magnetic stimulation.

Further, when the arachnoid is opened, the resulting brain shifts irreversibly, progressively compromising the reliability of both virtual models of AR systems and neuronavigation. This problem was recently addressed by manually optimizing the overlay of the virtual model in the surgical microscope. It has been reported,[70] that when severe deformation occurs during advanced tumor resection, compensation of any sort becomes impossible because of the parenchymal deformation. The brain shift problem could be dealt with by refreshing the virtual 3D models with intraoperative imaging, such as intraoperative MRI and intraoperative ultrasound, as with traditional neuronavigation systems.

2.3.4 Conclusions

AR represents a meaningful improvement of current neuronavigation systems. The prompt availability of virtual patient-derived information superimposed onto the surgical field view aids the surgeon in performing minimally invasive approaches. In particular, the large variety of technical implementations provides the neurosurgeon valid options for different surgeries (mainly neuro-oncological and neurovascular) for different treatment modalities (endovascular, endonasal, open), and for different steps of the same surgery (microscopic part and macroscopic part). Current literature confirms that AR in neurosurgery is a reliable, versatile, and promising tool, although prospective randomized studies have not yet been published.

Efforts should be invested in improving the AR systems setup, making them user friendly throughout all the different steps of the surgery (microscopic and macroscopic part) and across different surgeries. The virtual models need to be refined, perfectly merging with the surrounding real environment. Finally, new imaging techniques such as magnetoencephalography, transcranial magnetic stimulation, intraoperative MRI, and intraoperative ultrasound have the potential for providing new details for virtual models and improved registration.

3. Aim of the Study

AR in neurosurgery is a promising frontier; even if the AR systems tested in vivo up-to-date revealed several limitations both from the ergonomic and informational viewpoint[6, 7, 57-66]. The aim of this work is to investigate the effectiveness of a new highly ergonomic, easy-to-use, and cost-effective AR system based on a head mounted stereoscopic video see-through display (HMD) as an aid in complex neurological lesion targeting, namely a frontal tumor adjacent to the Broca's area. The ergonomics and usefulness of the HMD system were preliminary tested on a newly designed patient-specific head phantom, by 2 operators with different levels of neurosurgical training.

4. Materials and Methods

In this section, we provide a detailed description of the experimental set-up including the HMD system and the patient-specific head phantom that was designed as testing platform for our AR-based neuronavigation system. Further, we briefly outline the video marker-based method implemented for solving the image-to-patient registration problem.

4.1 System Overview

Our stereoscopic video see-through HMD for AR-based neuronavigation comprises the following two major components (Figure 8): a commercial 3D visor (Sony HMZ-T2) provided with dual 720p OLED panels and a horizontal field of view of 45°; 2 external USB cameras (IDS uEye XS) equipped with a 5 Megapixel CMOS sensor (pixel size of 1.4 μm) that achieve a frame rate of 30 fps at 1280x720 resolution. As previously described,[86-88] the two external cameras are mounted on the visor aligned with the user's eyes as to provide a quasi-orthoscopic view of the surgical scene mediated by the visor (in a video see-through fashion). The AR application was implemented in custom-made software library built in C++ on the top of the multipurpose EndoCAS Navigator Platform modules.[88] The management of the virtual 3D scene was carried out through the open-source software framework OpenSG 1.8 (www.opensg.org), while regarding the machine vision routines, needed for implementing the video-based tracking method, we adopted Halcon 7.1 software library developed by MVTec®. The whole system runs on a gaming laptop Alienware® M14 provided with an Intel Core i7-4700 @ 2.4 GHz quad core processor and 8 GB RAM. The graphics card is a 1GB nVidia® GeForce GTX 765M.

4.2 Video see-through paradigm

Here is a functional and logical overview of the video see-through paradigm underpinning our AR mechanism: the two external cameras grab video frames of the real scene; the video frames are screened as backgrounds onto the corresponding display of the visor; the software application elaborates the grabbed video frames to perform the real-time registration of the virtual content, defined during the surgical planning, to the underlying real scene (Figure 9).

The accurate patient-to-image registration is the fundamental prerequisite for yielding geometric coherence in the AR view of the surgical scene. This condition is satisfied if the virtual content of the scene is observed by a couple of virtual viewpoints (virtual cameras) whose processes of image formation mimic those of the real cameras in terms of intrinsic and extrinsic parameters. In this regard, the stereo rig calibration, which encompasses the estimation of the projective parameters of both cameras (i.e. intrinsic parameters) as well as the estimation of the relative position and orientation (pose) between the two cameras, is performed offline by implementing a standard calibration routine[89].

The online estimation of the transformation matrix $[R|T]$, which encapsulates the pose of the stereo rig reference system (CRS) in relation to the reference system of the surgical planning (SRS), is the result of a marker-based video registration method.[86, 90] This video-based tracking modality relies on the localization of at least three physical markers rigidly constrained to the head phantom and whose position in the virtual scene (SRS) is recorded during planning.

The key characteristic of the implemented method for registering the preoperative planning to the live views of the surgical scene (i.e. the patient phantom) is that it is not based on the adoption of a cumbersome external tracker. Standard surgical navigation systems, featuring the use of external infrared trackers, may in fact introduce unwanted line-of-sight constraints into the operating room as well as add error-prone technical complexity to the surgical workflow.[91] Our video-based algorithm provides sub-pixel fiducial registration accuracy on the image plane.

4.3 Surgical Planning

To assess the usefulness and ergonomics of our AR-based surgical navigation system we conducted preliminary tests on an Acrylonitrile butadiene styrene (ABS) replica of a patient-specific head phantom. From a surgical standpoint, we tested our system in a simulated high-risk neurosurgical scenario: the resection of a small tumor (or tumor portion) medially adjacent to the posterior part of the inferior frontal gyrus, where the Broca's area is generally located.

The 3D virtual models of the anatomical structures were the result of the segmentation of the preoperative computed tomography (CT) dataset: the DICOM files were segmented using a semi-automatic segmentation tool integrated into the open-source platform Insight Segmentation and Registration Toolkit.[92] The resulting 3D virtual anatomic details of the head, in the form of a STL file, were exported to a CAD software to layout the rigid parts of the 3D patient phantom (see section below).

The rendering of the anatomical details consisted of: skull base, skull cap before craniotomy, skull cap after planned craniotomy, lesions, and eloquent areas.

The 3D rendering of all the anatomically relevant structures of the head together with the purely geometrical elements and the synthetically created anatomical structures were individually exported to a 3D graphics-modelling tool (Deep Exploration by Right Hemisphere) to elaborate the surgical planning (Figure 10).

4.4 Experimental set-up: phantom realization

An experimental setup was appositely developed to test the whole system. The need for an effective evaluation of the AR platform was for a setup portraying at least: patient skin, skull, brain parenchyma, eloquent area/s and lesion/s. Such system allows for the simulation of skin incision, craniotomy and lesion reaching tasks both with a standard surgical approach and an AR-guided approach.

The set-up is showed in Figure 11. The whole anatomical structure except for the skin, lesions and eloquent areas was obtained from the segmentation of an anonymized CT dataset (1.25 slice thickness).[92, 93] The skull base and brain container, once segmented, was exported to a CAD software (PTC® CREO) where the model was modified. In a real setup, the reference markers needed for the tracker-less registration, should be put along the Mayfeld® U-shaped skull clamp. Therefore, we added four shelves around the skull as housing structures for the spherical markers.

Further, we added an array of housing holes along the skull basal surface that could hold the lesions and the eloquent areas in a predetermined position. This is a fundamental prerequisite to guarantee coherence between virtual and real environment. The obtained model was then printed with a 3D rapid prototyping machine (Stratasys® Elite Dimension). The fluorescent dyed spherical markers and the skull base are shown in Figure 11A. The synthetically created tumors and eloquent areas were printed separately and thereafter anchored to the skull basal surface in positions defined during surgical planning.

The skull cap, still obtained through segmentation, was 3D printed and thereafter a mould was created with the Mold Max® Performance Silicone Rubber (Smooth-On Inc.). The mould was used to reproduce the skull cap by a ceramic clay. Such a choice allows the consistent reproduction of all the skull caps needed for intensive testing. We carefully selected a type of ceramic dental clay that ensures good detail reproduction and provides a correct mechanical feedback during craniotomy (Figure 11B). As for the brain parenchyma the needs were threefold: (1) to reproduce brain sulci and gyri in order to provide realistic anatomical landmarks, (2) to reproduce brain consistency and elasticity for the lesion excision task, and (3) to determine a procedure that allows for relatively quick fabrication of several brains for

repeated tests. As for the first requirement, a mould was generated starting from the brain segmentation; the negative of the segmented 3D model of the brain was elaborated in the aforementioned CAD software; thereafter a bivalve mould was designed and 3D printed. As regards the second and third requirements, we selected a non-toxic durable material easy to handle in order to be able to reproduce brain phantoms for intensive testing. The selected material was a PVA-C -based hydrogel.[94, 95] A variety of PVA samples were produced with different PVA concentration and different numbers of freezing thawing cycles before reaching a consistency and elasticity that could meet clinical needs. Clinicians qualitatively assessed the different samples and chose a composition of a 4% PVA-H2O solution concentration with 4 Freezing/Thawing cycles to obtain the desired consistency and elasticity. In Figure 11C the resulting brain parenchyma comprising the main sulci and gyri is depicted.

The skin was obtained using Ecoflex® Silicone Rubber (Smooth-On Inc.). The clay skullcap was hand coated with three layers of approximately 0.5 mms/each. Figure 11D shows the complete "closed" phantom.

4.5 Preliminary testing

Details on the preliminary laboratory testing conducted at the EndoCAS center of the University of Pisa are presented in the following paragraphs.

The goal of these trials was to provide a preliminary evaluation of the effectiveness of our AR-based neuronavigation system as an aid into the definition of the optimal surgical corridor to reach the target and avoid the eloquent area (Figure 12). Thus, two surgeons were required to perform the same neurosurgical procedure on the left and right side of the patient-specific head phantom, respectively without and with the AR guidance.

When the experiment was conducted without AR, the surgeon was asked to reach the tumor and avoid the eloquent area, by properly tailoring the skin incision, osteotomy and cortical dissection, relying just on preoperative images and on the anatomical landmarks replicated in the phantom.

Otherwise, when the experiment was conducted with the AR guidance, the determination of the optimal surgical access to the surgical target was aided by providing the AR visualization. The definition of the virtual content to assist the skin incision, the craniotomy and the parenchymal corridor was elaborated during the surgical planning relying on the data derived from the segmentation of the CT dataset.

5. Results

With the aid of our AR visor, both the surgeons were able to navigate to the target lesion on the basis of the AR visualization modalities above described. Initially, all the virtual content was presented to the operator, in order to provide an overall understanding of the surgical planning overlaid to the real surgical field. Then, the AR modalities dedicated to the execution of the specific surgical subtasks, were stepwise provided to the surgeon, according to the steps of a traditional procedure of brain tumor resection. Therefore, as a first step, the perimeter of the skin incision was shown. After the skin was accordingly incised, the virtual incision contour was substituted in the AR scene by the perimeter of the craniotomy. Finally, the determination of the optimal dissection corridor for accessing the lesion as well as for avoiding the eloquent area was aided by means of the AR visualization modality "*Anatomical Occlusions and Transparencies"*.

The surgeons could orient the dissecting instrument (resembling bipolar forceps) and navigate to the surgical target relying on their augmented 3D perception of the surgical field. The mutual integration between occlusions, motion parallax, and stereopsis allowed the surgeon to perceive the relative proximities between tumour, eloquent area and surrounding brain parenchyma.

The two surgeons performed the same task on the contralateral side of the brain without the aid of the AR view. At the end of both the experiments the surgeons qualitatively compared the two approaches. As for the skin incision subtask, the AR guidance allowed an evident reduction on the size of the incision (Figure 13A and 13D). A similar result was obtained on the craniotomy subtask: the use of the AR visualization proved to be an effective aid in tailoring the craniotomy that, otherwise, would be defined on the basis of the skull bony landmarks (Figure 13B and 13E). Finally, the optimal trajectory for accessing the lesion was improved by means of the AR guidance (Figure 13C and 13F). Such approach complements the surgeon's anatomical knowledge of the brain surface with additional and intuitive real-time information. It is important to outline that the reported results do not intend to have any statistical significance yet they strongly encourage to conducting a more structured study. Nonetheless, the testing platform was

qualitatively judged as very realistic and worthy of being utilized also for training purposes in combination or separately to the AR neuronavigator.

6. Discussion

The HMD-based AR systems has been used in a variety of surgical specialties including, but not limited to, general surgery,[96] vascular surgery,[97] maxillofacial surgery,[98] and very rarely in neurosurgery.[68] Nonetheless, neurosurgery is a special challenge, as well as a unique opportunity for any AR system development, because any inaccuracy in registration or image display might result in relevant morbidity and mortality. Additionally, the concept of minimally invasive neurosurgery mandates the smallest possible approaches for a given pathology.[55] Consequently, the neurosurgeon is often required to work in deep and narrow corridors, surrounded by critical nervous and vascular structures. Thus, the ideal AR-implemented virtual models must show several different anatomical details in a very limited space, in a stereotactic manner (preserving depth perception), perfectly merging with the actual surgical field, with perfect virtual-real registration accuracy, and without hiding the actual anatomy underneath.

We attempted this difficult challenge by testing the limits of a HMD-based AR system in a simulated high-risk neurosurgical scenario: the resection of a small tumor (or tumor portion) medially adjacent to the posterior part of the inferior frontal gyrus, where the Broca's area is generally located.

In a similar fashion to the current neuronavigation systems, a traditional preoperative planning was prepared. In our experiment, two areas were identified, the tumor and the eloquent area (Broca's), as they can be seen on a MRI, or fMRI, scan. From the relative position of the target and the eloquent area, the surgical trajectory, the site of the craniotomy and of the skin incision were sequentially and logically deducted, creating coherent virtual models. Although our study did not provide any statistically significant data because of tests shortage, nonetheless it suggests 3 major conclusions: first, our AR system is intuitive, second, it is very useful to reach even small lesions while avoiding adjacent eloquent areas, third, that it might be also used for training purposes. Thus, our system qualifies to be a useful tool to be tested in vivo when performing neuro-oncological procedures.

From a technical viewpoint, our AR system overcame some limitations not only of the neuronavigation systems, but also of several different AR systems previously applied to Neurosurgery. First, because the

HMD has two separate cameras for recording and image injection, both the virtual objects and the surgical field are show in 3 dimensions. Conversely, the neuronavigation systems present just the virtual plan as 3 perpendicular planes of bidimensional images. As a consequence, 3D relationship between the target and eventual other anatomy details needs to be mentally reconstructed by the surgeon. Additionally, the system appears to be poorly ergonomic and potentially harmful, because the operator, while introducing the bayonet pointer in the operating field, has to look away from the surgical field itself, toward the workstation screen. None of the other AR systems applied to neurosurgery is able to present a 3D virtual model overlaid on a 3D environment. In fact, AR systems relying on the injection of virtual images in the operating microscope can show virtual 2D or 3D objects overlaid on a 2D environment.[58, 59, 62, 63, 66] Such a limitation is common to AR systems based on head-held[7] or hand-held cameras. The most famous of these systems, the Dex-Ray, is composed by a lipstick-shaped hand-held tracked camera that serves as source images about the real surgical field. The virtual images are overlaid on the environmental recorded images on a remote screen.[6] Thus, also in this set-up, the final image is bidimensional and, additionally, the neurosurgeon has to look away from the surgical field while introducing a pointer in the field.

Although the HMD-based AR system theoretically overcomes the problem of 3D virtual and real images, nonetheless the operators participating to the experiment reported that still the depth perception is suboptimal. In fact, from a practical viewpoint, the virtual objects do not fully merge with the real environment, and appears slightly to "jump out" from the surgical scene, although less remarkably than in previous studies.[6, 63, 99]

Although several methods were proposed in order to improve depth perception,[85] one of the simplest and more intuitive tools is to adjust color coding depending on object depth. As an example, superficial objects can be rendered as clear and bright, while deeper structures foggy and opaque. Another limitation of almost, if not all, AR systems, including ours, is the lack of tracked surgical instruments. In fact, when a tracked instrument approximate the lesion, a section of the surgical target itself, corresponding to the hidden portion by the instrument, could be subtracted in the final image, exactly replicating how a shadow hides objects in the real world. Of course, instrument tracking is a very time consuming task and it might be also unpractical. In fact, additional tracking reference hardware needs to be positioned on the instruments, potentially resulting in further reduction of the field of view. In our virtual model,

viewfinders were created in order to refine the orientation of the dissecting instrument toward the lesion, as well as away from the eloquent region. Although this technical expedient does not completely resolve the problems with depth perception, nonetheless, it is a practical, easy-to-build and intuitive tool for improving operator's confidence, as confirmed by the opinions of the two neurosurgeons.

Another critical aspect affecting depth perception is the parallax problem: when the point-of-view of the surgeon is the same of the optical device, there is no mismatch between what the operator sees and what the device actually captures. Conversely, when the operator and the optical device have different point-of-view, uncertainty might raise on the actual position of the target. Thus, as an example, parallax problem affects the AR systems relaying on a handheld video probe (Dex-Ray)[6] and systems that use a video projector for AR presentation.[99] Conversely, when AR is injected in the surgical microscope the optical focus itself becomes the actual navigation pointer.[63] In a similar fashion all the see-through systems, including ours, are characterized by being interposed between the operator's eye and the surgical field. Thus, the line of view of the operator perfectly matches the one of the AR system, regardless whether the device is wearable,[7] or not.[65]

Another crucial aspect of the introduction of an AR system in daily practice is the cost effectiveness. In the case of AR systems based on the surgical microscope, the necessary equipment (including the neuronavigation system to track the microscope) is promptly available in most of the modern operating rooms. Thus, their introduction in daily practice would not require additional costs. Conversely, in developing countries, such a highly technological equipment is exceedingly expansive. Some AR set-up are cheaper than a standard neuronavigation system, and potentially might replace them, although with evident limitations, as demonstrated in case of a very rudimental AR system, composed by a 3D rendering software and a digital camera.[60] Our HMD-based system cost about 1000 dollars, and do not require a standard neuronavigation system. So, it might be an affordable option in any economic situation.

As demonstrated for the largest part of the AR system,[6, 60, 65, 70, 74, 99] the HMD-based AR system is a valid tool in the "macroscopic" part of the intervention, including skin incision, craniotomy, dural opening and lesion targeting. Nonetheless, all these systems do not seem to be useful for microsurgical tasks. Conversely, although with several limits in 3D visualization and depth perception, microscope-based AR systems were reported as beneficial for tumor[100] or AVM resection,[62] aneurysm clipping,[63] by-pass

creation.[66] On the other hand, it is common experience that the microscope is quite unpractical when the macroscopic part is performed.

Thus, we acknowledge that all the AR systems, have an ideal field of application (macroscopic, microscopic, neurovascular or oncological), and any comparison should be done between systems aiming to the same task.

The limitations and future directions of our study consist in the limited number of experiments performed and the approach in vitro itself. Additionally, there is still margin to improve depth perception, both by improving the semantics of virtual objects as well as tracking instruments. Then, the next challenge for any AR system should the possibility of intraoperative plan updating. In fact, as the tumor resection goes on, the brain shift and deformation make preoperative planning gradually less useful. The use of intraoperative imaging should be used to refresh virtual objects' shape and position.

Finally, although only MRI was used in the present study, other new imaging techniques should be used, including magnetoencephalography, transcranial magnetic stimulation, tractography, since the AR systems represent an ideal platform for multimodal image fusion.

7. Conclusions

When compared to similar systems,[6, 60, 65, 70, 74, 99] the HMD-based AR neuronavigation system herein presented proved: to provide an unpreceded 3D visualization both of the surgical field and of the virtual objects, to provide an improved depth-perception of the augmented scene, to be ergonomic and unaffected by the parallax problem, to be very cost-effective, to be a useful tool for the macroscopic part of neuro-oncological procedures. Further, our testing platform might be used for training purposes, in combination or separately to the AR neuronavigator. Finally, the preliminary results herein presented strongly encourages to conducting a more structured study to prove its clinical effectiveness.

Author	Date	Subspecialty	Lesions	Pathology/ location	Real data source	Virtual data source	Tracking modality	Registration technique	Visualization processing	Display type	Perception location
Doyle W.K.	1996	NO (Epilepsy)	40	N/A	See Visualization Processing and display type	CT, MRI	Magnetic tracker	Fiducial markers and others (N/A)	Standard Nav. view: MRI slices + pointer	PC monitor or semitrans. head-up display	Stand up or semitrans. head-up display
Iseki H. et al.	1997	NO/NV	6	Glioblastoma/ frontal x2, Hematoma/ frontal, Meningioma/ frontal, Meningioma/ ventricle, Meningioma/ skull base,	Unaided view of the patient	CT, MRI	None	Manual	Light field rendering	Light field display and half mirror at 45°	Patient
Masutani Y. et al.	1998	NV (endovascular)	3	Aneurysm MCA, Aneurysm MCA+ basilar apex	X-ray fluoroscopy	CTA, MRA	None	Fiducial markers	Texture maps	Monitor	External monitor
King A.P et al.	1999	NO/NV	4	Cyst/bilateral petrous apex, AVM/ central sulcus, Unknown lesion/ facial nerve,	Microscope	CT, MRI	Optical tracker	Skull or dental-fixed fiducials	Wireframe and texture maps	Microscope oculars (via a beam splitter)	Patient
Kawamata T. et al.	2002	NO	12	Adenoma/ pituitary x12	Endoscope	CT, MRI	Optical tracker	Fiducial markers	Wireframe and color map (code color-distance)	Monitor	Endoscope monitor
Edwards P.J. et al.	2004	NO/NV	17	AVM /cortical superficial, Meningioma/ clivus, Meningioma / parietal, Meningioma/ subfrontal x2, Meningioma / ethmoidal, Schwannoma/ vestibular x2, Epidermoid, Jugular glomus tumor, Neuroblastoma/olfactory Carcinoma/ ethmoidal x3, Unknown lesion/ carotid, Cystic lesion /petrous apex, Angioma/ facial nerve,	Microscope	CT, MRI	Optical tracker	Skull or dental-fixed fiducials	Wireframe and texture maps	Microscope oculars (via a beam splitter)	Patient
Paul P. et al.	2005	NO/NV	6	Cavernoma/ frontal. Cavernoma/ temporal, Cavernoma/ central. Glioma/ frontal x3	Microscope	MRI, fMRI, MEG	Optical Tracker	Manual, fiducial markers, skin surface	Texture maps	Monitor of Nav.	Monitor of Nav.
Lovo E.E. et al.	2006	NO/NV/ nNO-nNV	8	Glioblastoma/ parietal, Ependymoma /ventricle Metastasis/ frontal, Hydrocephalus, Neuroepitelial tumor/ temporal, Infarct/ cerebellar Oligodendroglioma/ temporal, Hemangioblastoma/ cerebellar	Hand-held digital camera	CT, MRI, MRA	None	Manual	Transparencies	Monitor	Stand up monitor
Stadie A.T. et al.	2009	NV	16	Cavernoma/ unknown x16	Microscope	CT, MRI	Optical tracker	Skin surface (face)	Surface mesh	Microscope eye-piece	Patient
Kockro R.A. et al.	2009	NO/NV	12	Meningioma /petroclival, Meningioma /sphenoidal, Meningioma /falcine x2, Glioma /parietal, Glioblastoma /frontal,	Lipstick-shaped video-camera	CT, MRI, MRA	Optical tracker	Manual (refined by moving the tracked camera)	Transparencies	Monitor	Stand up monitor

				Glioblastoma /temporal, Glioblastoma /frontoparietal, Metastasis /cerebellar, AVM /cerebellar, Aneurysm /PICA Cavernoma /occipital							
Low D. et al.	2010	NO	5	Meningioma/ falcine Meningioma/ parasagittal x3 Meningioma/ convexity	Lipstick-shaped video-camera	CT, MRI, fMRI, MRA	Optical tracker	Manual (refined by moving the tracked camera)	Transparencies	Monitor	Stand up monitor
Inoue D. et al.	2013	NV	3	Meningioma/ convexity x2, Glioblastoma/corpus callosum	Handheld or headheld camera	CT, MRI, tractography	Optical tracker	Fiducial Markers	Surface mesh (3D)	Monitor	Stand up monitor
Deng W. et al.	2014	NO	3	"Tumors"/unknown x3	Tablet camera	CT, MRI	Optical tracker	Fiducial Markers	Surface mesh (3D), transparencies	Tablet monitor	Patient through tablet
Cabrilo I. et al.	03/ 2014	NV	39	Aneurysm/ Int. Carotid x3 Aneurysm/ Acomm x8 Aneurysm/ MCA x21 Aneurysm/ Pcomm x5 Aneurysm/ PCA Aneurysm/ SCA	Microscope	MRA, CTA, Angiography	Optical Tracker (Nav.)	Skin surface (face)	Surface mesh (or surface contours)	Microscope eye-piece	Patient
Cabrilo I. et al.	07/ 2014	NV	5	AVM/frontal AVM/parietal AVM/temporal AVM/ occipital AVM/ insular	Microscope	MRA, CTA, Angiography	Optical Tracker (Nav.)	Skin surface (face)	Surface mesh (or surface contours)	Microscope eye-piece	Patient
Cabrilo I. et al.	2015	NV	4	Moya-Moya/STA-MCA x3 Vertebral art. dissection/ Occipital art-PCA	Microscope	MRA, CTA, Angiography	Optical Tracker (Nav.)	Skin surface (face)	Surface mesh (or surface contours)	Microscope eye-piece	Patient
Kantelhardt S.R. et al.	2015	NO	7	Metastasis/ frontal x3 Glioma/ temporoparietal Metastasis/ parietal x3	Microscope	CT, MRI	Optical tracker	Skin surface (face)	Surface mesh	Microscope eye-piece	Patient
Besharati Tabrizi L. et al.	2015	NO	5	Metastasis/ supratentorial x3 Glioblastoma/ supratentorial x2	Unaided view of the patient	CT, MRI	None	Manual	Surface mesh	Projector	Patient

Acomm, anterior communicating artery; AVM, arterovenous malformation; CTA, angio-CT; MCA, middle cerebral artery; MEG, magnetoencephalography; MRA, angio-MRI, Nav, neuronavigator; NO, neuro-oncology; NV, neurovascular; nNO-nNV, non neuro-oncology non-neurovascular; Pcomm, posterior communicating artery; PCA, posterior cerebral artery; SCA, superior cerebellar artery; semitrans, semitransparent.

Table 2. Neurosurgical lesions treated with the aid of Augmented Reality

PATHOLOGY	# LESIONS	% LESIONS
Neoplastic lesions	**75**	**38.46**
Glioma/GBL supratentorial[6, 7, 60, 64, 70, 71, 99]	14	7.17
Glioma/GBL infratentorial	0	0
Meningioma/supratentorial[6, 7, 59, 64, 74]	12	6.15
Meningioma/infratentorial-skull base[6, 59, 64]	7	3.58
Pituitary adenoma[57]	12	6.15
Metastasis[6, 60, 70]	11	5.64
Schwannoma, vestibular[59]	2	1.02
Ependymoma[60]	1	0.51
Oligodendroglioma[60]	1	0.51
Hemangioblastoma[60]	1	0.51
Neuroepitelial tumors[60]	1	0.51
Other neoplastic lesions[58, 59, 65]	13	6.66
Vascular lesions	**77**	**39.48**
Aneurysm ant.circul.[61, 63]	39	20.00
post.circul.[6, 63]	4	2.05
Cavernoma[6, 69, 71]	20	10.25
AVM[6, 58, 59, 62]	8	4.10
Moya-Moya disease (by-pass)[66]	3	1.53
Stroke[60, 64]	2	1.02
Arterial dissection (By-pass)[66]	1	0.51
Non-neoplastic, non vascular	**1**	**0.51**
Hydrocephalus[60]	1	0.51
Undetermined	**42**	**21.53**
Epileptogenic lesions*[68]	40	20.51
Others	2	1.02
Total	***195***	***100***

Ant. circul., anterior circulation; AVM, arterovenous malformation; GBL, Glioblastoma; post. circul., posterior circulation

***The Author reports these lesions as mainly oncological, although an histological classification (Tumor or vascular) of the treated cases was not provided.

Figures

Figure 1.

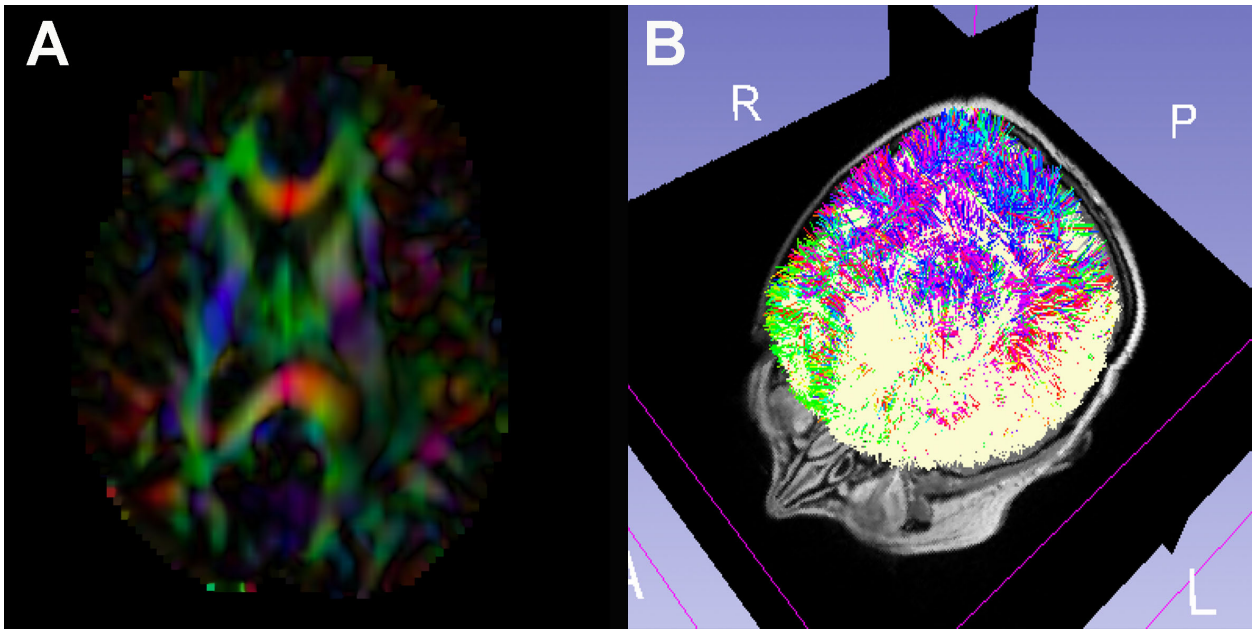

A tractographic reconstruction process. **A,** Color coded map of white matter connections in an axial slice of the brain. **B**, Three-dimensional reconstruction of all the fibers of the brain

Figure 2.

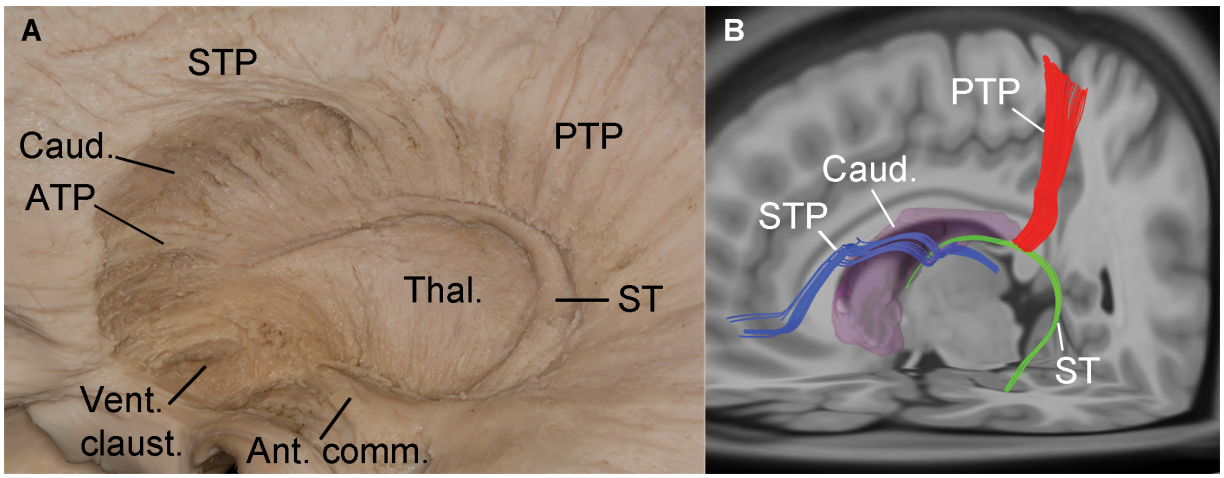

Lateral view of the STP, ST and PTP of the left hemisphere, depicted by anatomical dissection (**A**) and fiber tracking reconstruction (**B**). A and B show that the STP knees posteriorly on the superolateral aspect of the caudate nucleus (Caud.), and then arches inferiorly on the inferolateral side of the head and body of the caudate nucleus, reaching the thalamus (Thal.). Posteriorly and medially to the STP, the ST runs in the groove between the inferomedial aspect of caudate nucleus and superolateral aspect of the thalamus, then it knees inferiorly on the lateral aspect of the thalamus and finally courses anterolaterally toward the temporal horn of the lateral ventricle. A and B show no continuation between the fibers of the STP, ST and PTP (ATP, anterior thalamic peduncle; Vent. claus., ventral claustrum; Ant. comm., anterior commissure).

Figure 3.

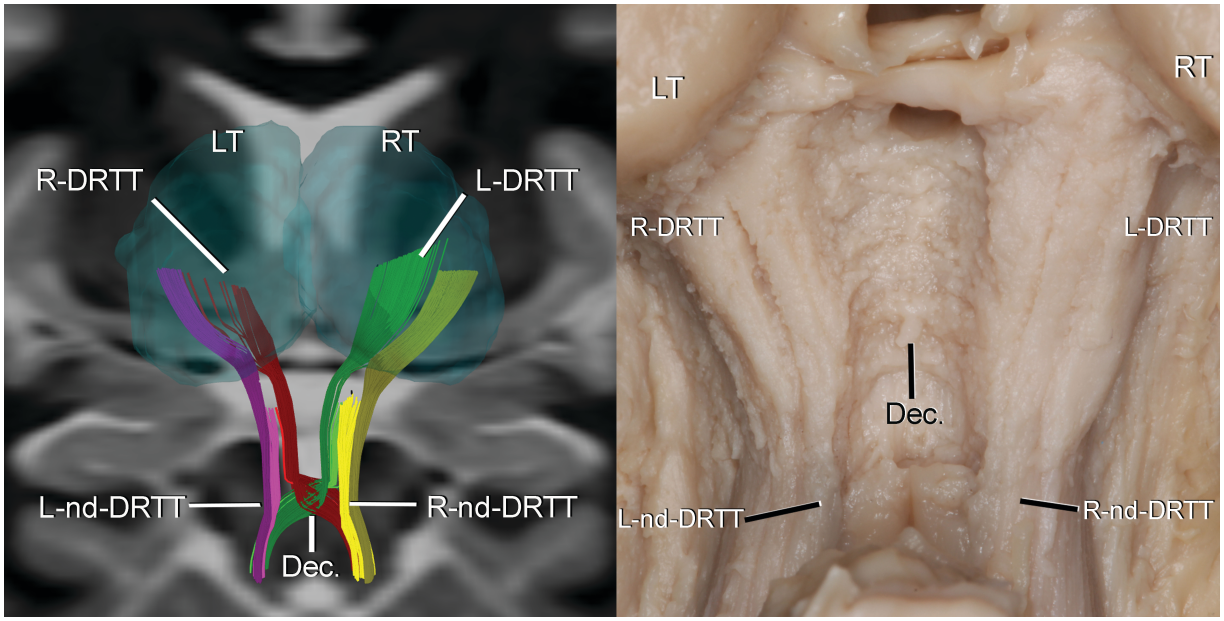

Bilateral dentatorubrothalamic system, depicted by fiber tracking reconstruction (left) and anatomical dissection (right). **Left:** The fibers arising from left are: the left nd-DRTT (L-nd-DRTT) containing the left nd-DRT (in light pink); the left DRTT (L-DRTT) containing the left DRT (in light green). The bundles arising from right are: the right nd-DRTT (R-nd-DRTT), containing the right nd-DRT (in light yellow); the right DRTT (R-DRTT), containing the right DRT (in light red). **Right:** The L-nd-DRTT and the R-nd-DRTT ascend dorsally and posteriorly to the R-DRTT and L-DRTT before and after their decussation (Dec.). In each DRTT, the more ventral the fibers are, the more caudal they are located in the decussation. (LT, left thalamus; RT, right thalamus)

Figure 4.

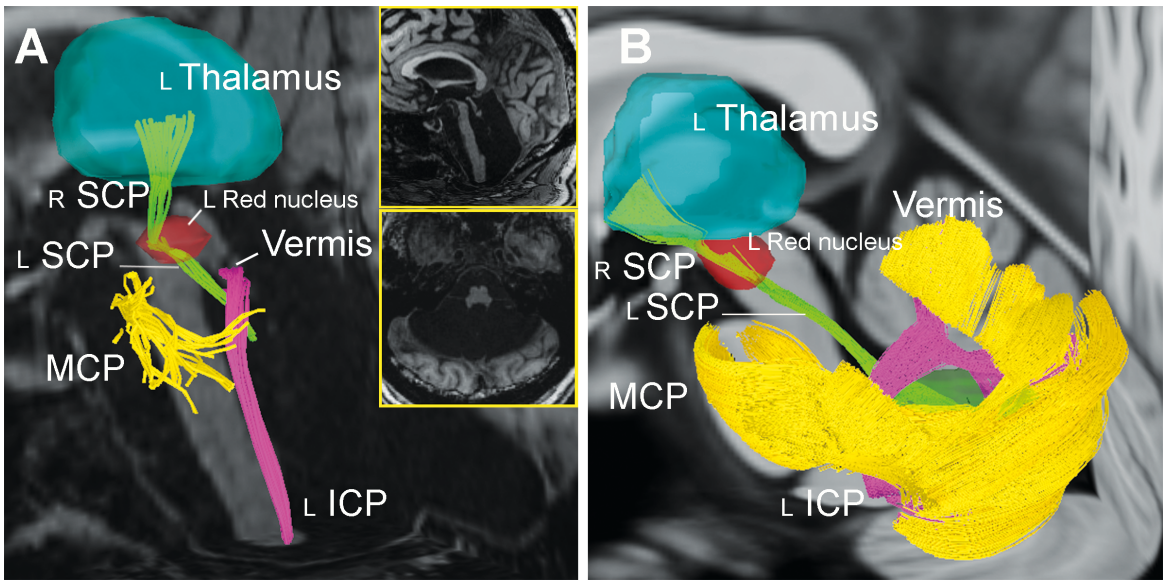

Tractographic analysis of the cerebellar peduncles in a case of cerebellar agenesis and in normal subjects. **A,** Tractographic analysis of the superior, inferior and middle cerebellar peduncles (respectively SCP, ICP, MCP). In the inserts: sagittal (above) and axial (below) T1-weighted MRI of the posterior fossa showing almost absent cerebellum. **B,** Tractographic analysis of the SCP, ICP and MCP (whose fibers were partially sectioned inside the cerebellum) in normal subjects. (L, left; R, right)

Figure 5.

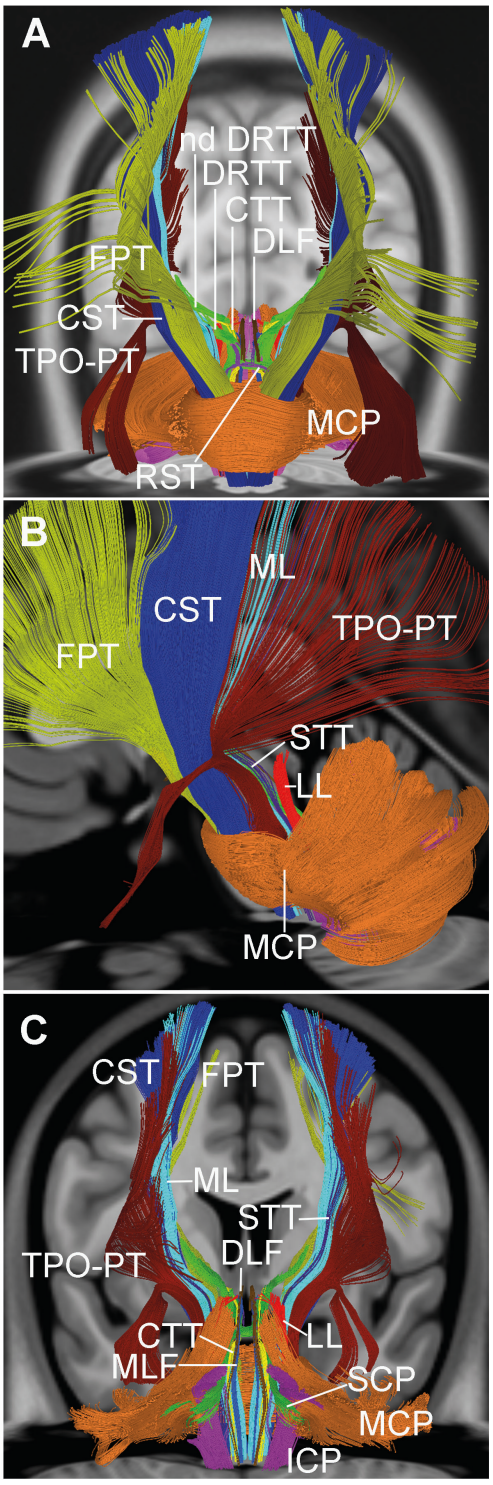

Comprehensive tractographic reconstruction of the brainstem tracts. **A,** Coronal anterior view. **B,** Sagittal left view. **C,** Coronal posterior view. (CST, corticospinal tract; CTT, central tegmental tract; DLF, dorsal longitudinal fasciculus; DRTT, dentatorubrothalamic tract; FPT, frontopontine tract; ICP, inferior cerebellar peduncle; LL, lateral lemniscus; MCP, middle cerebellar peduncle; ML, medial lemniscus; MLF, medial longitudinal fasciculus; nd DRTT, non decussating dentatorubrothalamic tract; RST, rubrospinal tract; STT, spinothalamic tract; SCP, superior cerebellar peduncle; TPO-PT, temporo-parieto-occipito-pontine tract).

Figure 6.

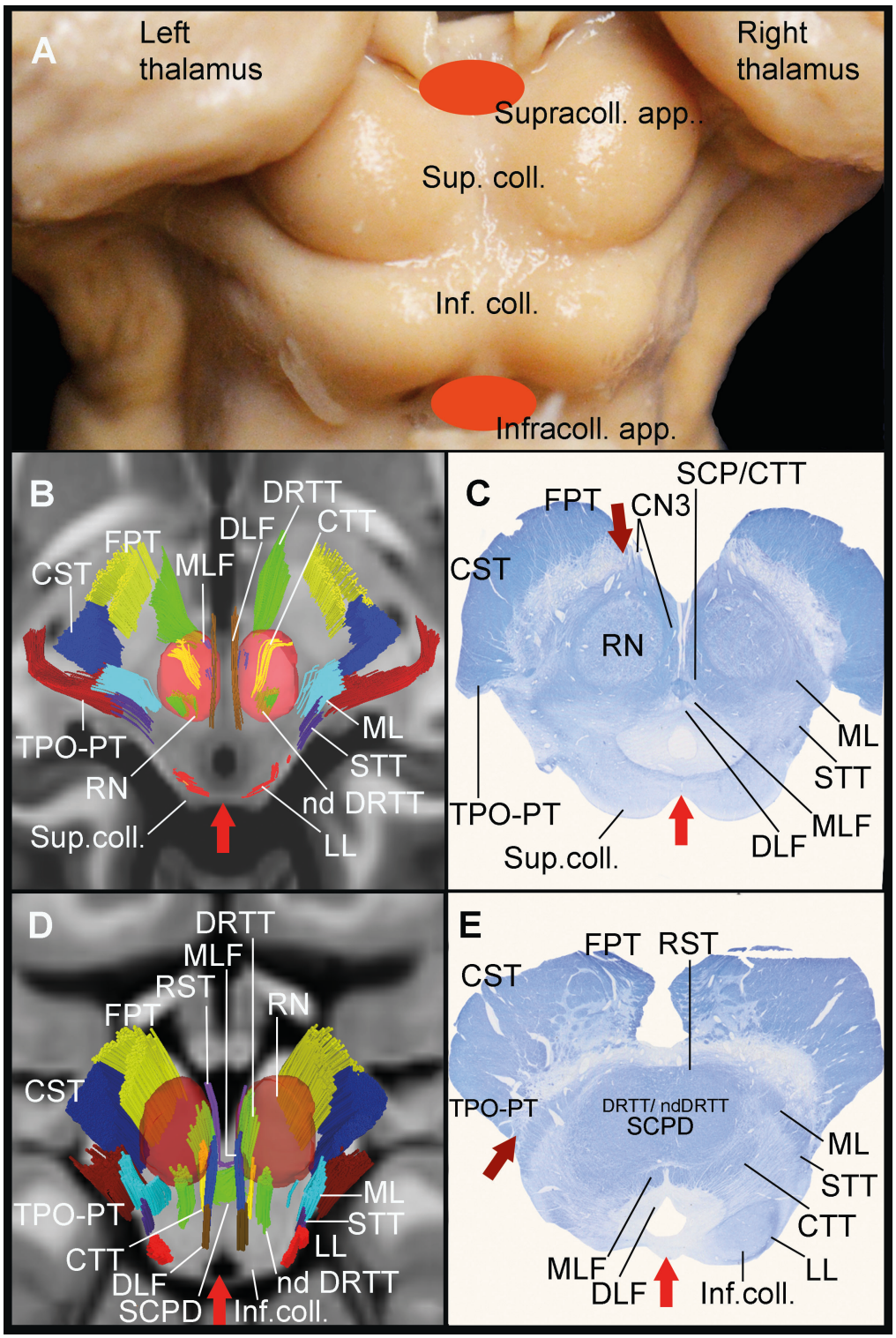

Sectional anatomy and surgical approaches to the dorsal midbrain. **A,** Overview of the dorsal approaches to the midbrain in a cadaveric specimen. The supracollicular approach (Supracoll. app.) is conducted dorsally to the superior colliculi (Sup. coll.) of the lamina quadrigemina. The infracollicular approach (Infracoll. app.) is performed caudally respect to the inferior colliculi (Inf. coll.). **B,** The supracollicular approach in a tractographic section. The axial plane is set at the level of the Sup.coll. As shown by the *red arrow*, the

approach is conducted cranially to the Sup.coll., above the upper termination of the lateral lemniscus (LL). The approach is limited anteriorly by the dorsal longitudinal fasciculus (DLF), the medial longitudinal fasciculus (MLF) (slightly ventral to the DLF) and, laterally to the DLF, by the red nucleus (RN) with its relative tracts, namely the non-decussating dentatorubrothalamic tract (nd DRTT), the decussating dentatorubrothalamic tract (DRTT) and the central tegmental tract (CTT). The lateral limit of the surgical corridor is formed by the medial lemniscus (ML) anteriorly, and the spinothalamic tract (STT) posteriorly. Anterolaterally to the red nucleus (RN), the cerebral peduncle is formed, from medial to lateral, by the frontopontine tract (FPT), the corticospinal tract (CST) and the temporo-parieto-occipito-pontine tract (TPO-PT). **C,** The supracollicular approach and the perioculomotor approach on a histological section. The cut is performed at the level of the Sup. coll. with a slight orientation from posterior and superior to anterior and inferior, showing the third cranial nerve (CN3). As in picture 5B, the supracollicular approach (*light red arrow)* is limited by the anterior wall of the cerebral aqueduct. In fact, from medial to lateral, the following tracts are found: the DLF, the CTT (at this level impossible to distinguish from superior cerebellar peduncle, SCP, fibers), the MLF, the ML and the STT. Anterolaterally to the RN, from medial to lateral the FPT, the CST and the TPO-PT are found. The perioculomotor approach *(dark red arrow)* is limited medially by the intraparenchimal course of the CN3 fibers, and laterally by the FPT. **D,** The infracollicular approach in a tractographic view. The axial plane is set at the lower limit of the Inf. coll. As shown by the *red arrow*, the approach is conducted caudally to the Inf. Coll. On the sagittal plane, from the surgical perspective, the cerebral aqueduct, the DLF, the MLF, the SCP decussation (SCPD) and the rubrospinal tract (RST) are found. Laterally to the MLF, from medial to lateral, there are the CTT, the nd DRTT and then the three tracts forming the lateral wall of the mesencephalic tegmentum, namely, from anterior to posterior, the ML, the STT and the LL. Thus, the approach is limited anteriorly by the DLF, the CTT and the nd DRTT, and laterally by the LL and the STT. **E,** The infracollicular approach and the lateral mesencephalic approach on histological section. The section is performed at the level of the Inf. coll. Accordingly with figure 5D, on the coronal plane, ventrally to the cerebral aqueduct, the DLF, the MLF, the SCPD (DRTT and nd DRTT are not distinguishable here) and the RST are stepwise found from posterior to anterior. The infracollicular approach *(light red arrow)* is limited laterally to the MLF, by the CTT and by the superficial tracts of the mesencephalic tegmentum (ML, STT and LL). The lateral mesencephalic approach *(dark red arrow)* is conducted trough the corresponding sulcus, between the TPO-PT, the CST and FPT anteriorly, and the ML and the SCPD posteriorly.

Figure 7.

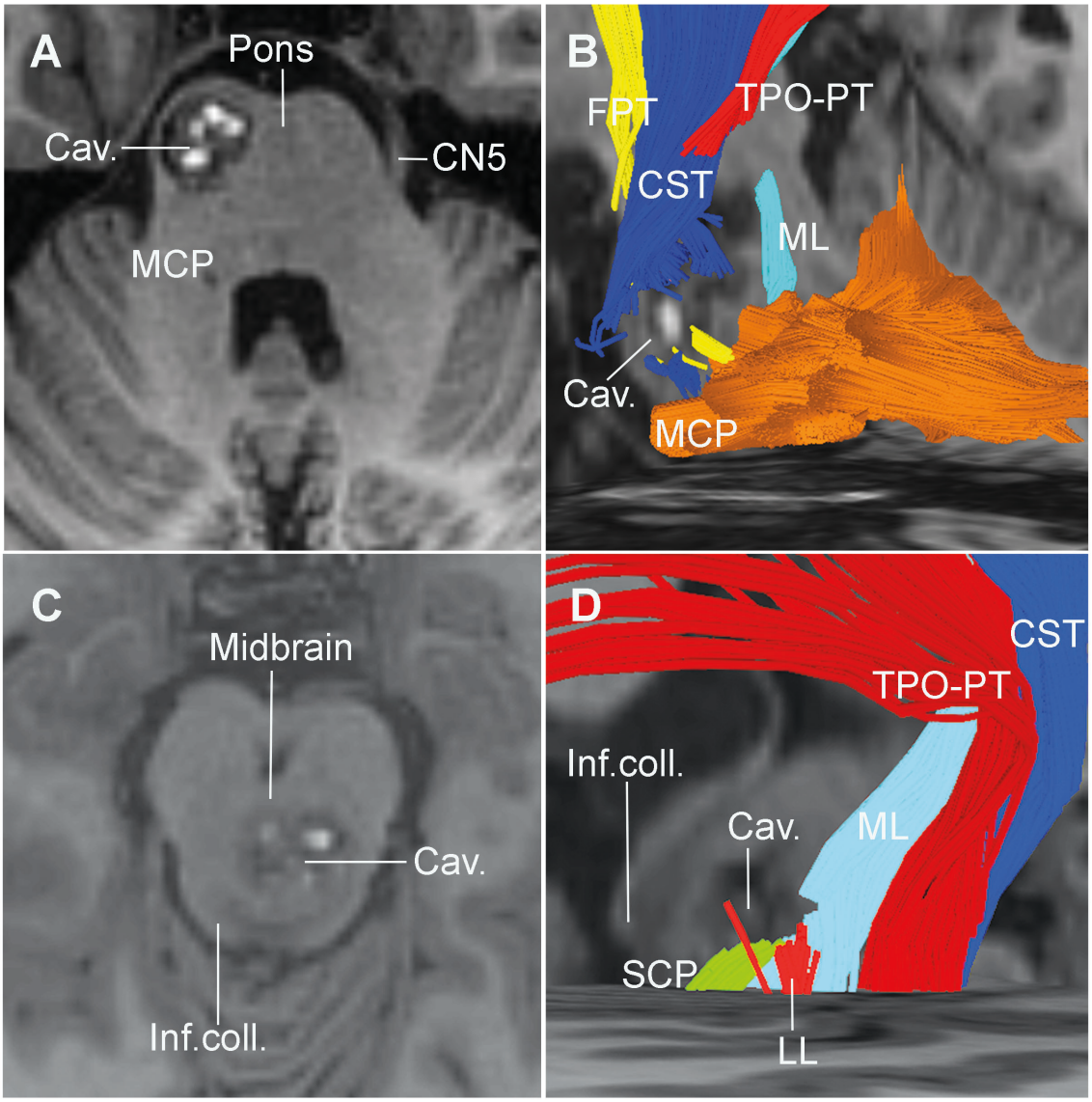

Clinical cases of brainstem lesions. A, Case 1. The axial T1-weighted MRI shows a bleeding cavernoma (Cav.) in the left ventral pons at the height of the fifth cranial nerve (CN5). B, Tractographic preoperative planning of case 1. The frontopontine tract (FPT), the corticospinal tract (CST) and the temporoparieto-occipito-pontine tract (TPO-PT) are partially injured and medially displaced by the cavernoma. The medial lemniscus (ML) is displaced posteriorly and medially. The cranial half of the transverse fibers of the middle cerebellar peduncle (MCP) are damaged opening the way for the surgical approach. C, Case 2. The axial T1-weighted MRI shows a bleeding cavernoma (Cav.) in the depth oh the right tegmentum of the midbrain, at the level of the inferior collicolus (Inf. Coll.). D, Tractographic preoperative planning of case 2. The cavernoma caused an interruption of the signal of the most posterior part of the ML, the upper termination of the lateral lemniscus (LL) and of the superior cerebellar peduncle (SCP) in its ascending course toward the decussation. Thus, the right lateral medsencephalic sulcus approach appears to be the safest option to resect the cavernoma.

Figure 8

The head mounted stereoscopic video see-through display

Figure 9

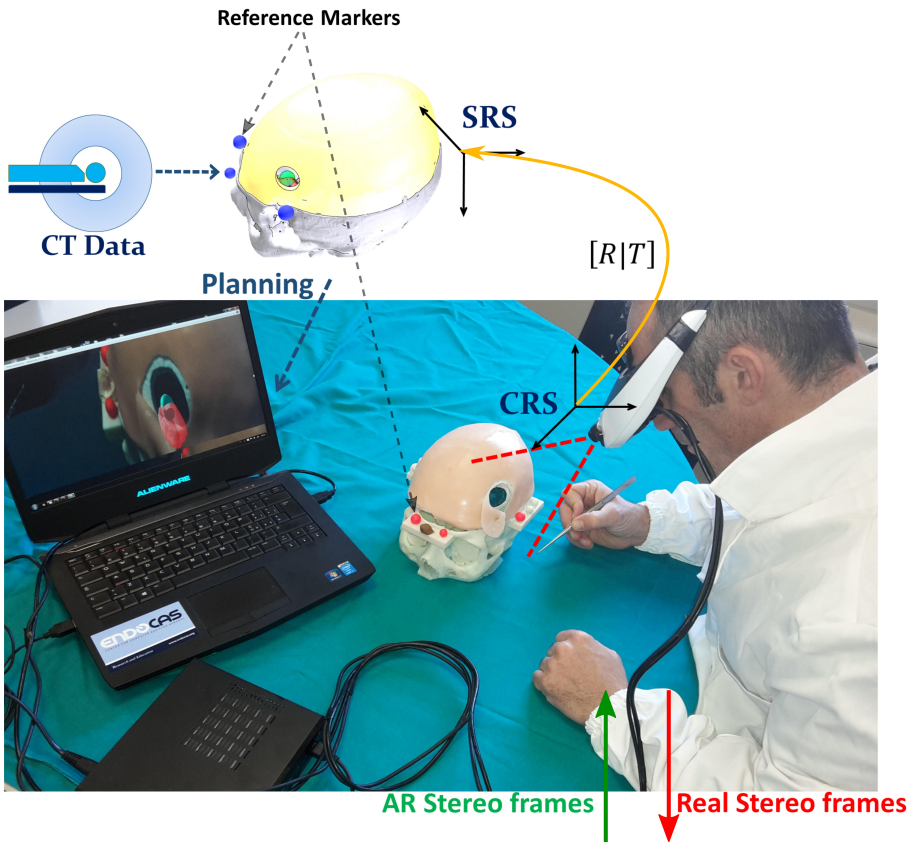

Video see-through paradigm of the augmented reality neuronavigator. The software application merges the virtual three-dimensional surgical planning with the stereoscopic views of the surgical scene grabbed by the stereo rig. Thereafter, the augmented reality stereo frames are sent to the two internal monitors of the visor. Alignment between real and virtual information is obtained by a tracking modality that relies on the localization of at least three reference markers rigidly constrained to the head phantom and whose position in the surgical scene (SRS) is recorded during planning.

Figure 10.

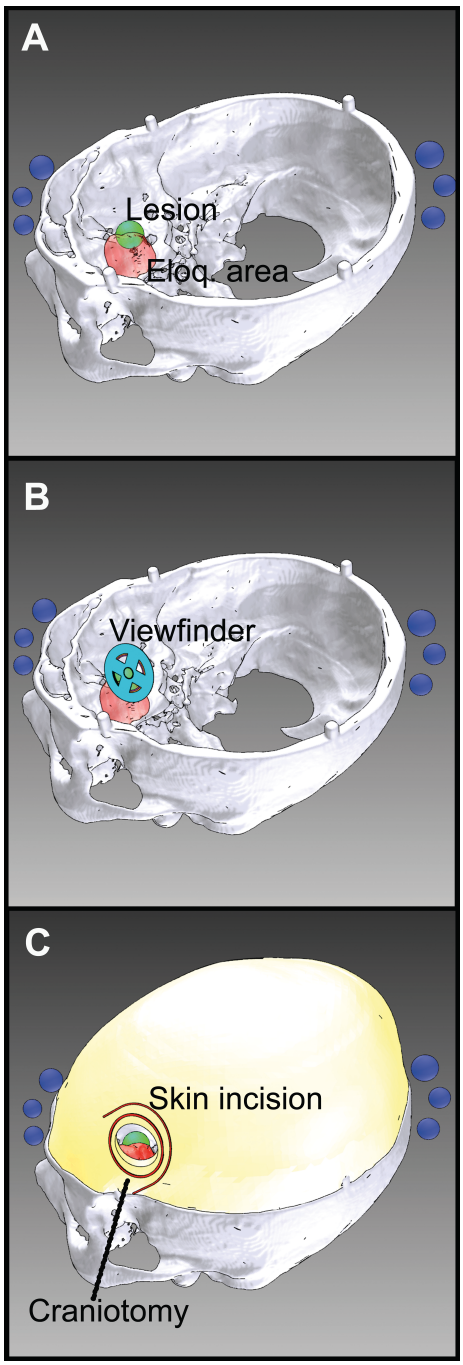

Surgical planning. A, Respect to the skull base, the neoplastic lesion is medial to the eloquent area (Eloq. area). B, A viewfinder is positioned superolaterally to the lesion, in order to determine the surgical trajectory through the brain. C, In the virtual model of the skull including the vault, the exact size and shape of the craniotomy and skin incision can be deducted on the basis of the surgical trajectory.

Figure 11.

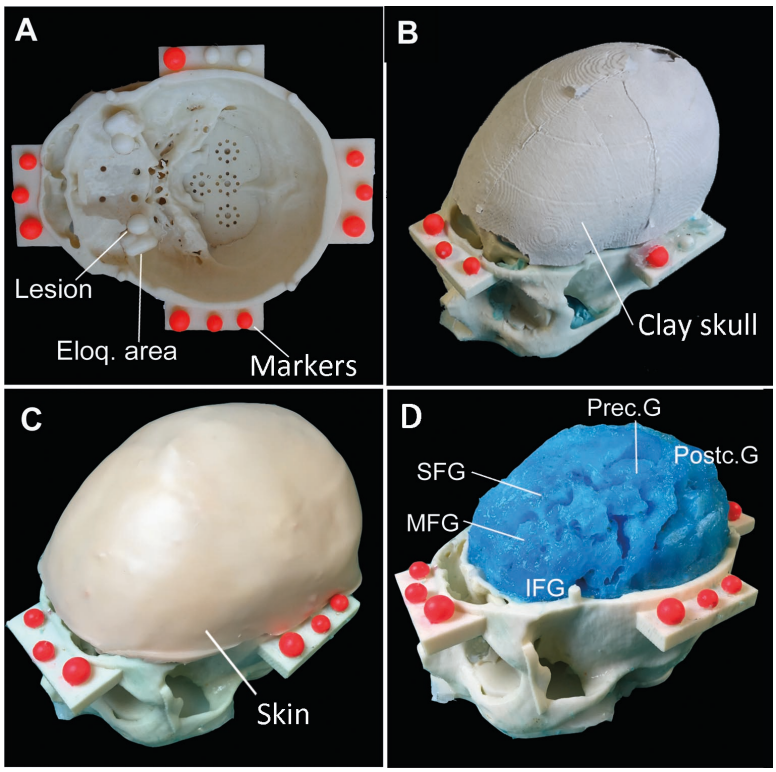

Structure of the phantom. A) The skull base is embedded with bilateral frontal lesions both medial to the adjacent eloquent areas (Eloq. area). The inner surface of the skull base presents several housing designed to insert further lesions or eloquent areas. Four lateral shelves served as support for optical reference markers (fluorescent dyed spheres). B) The skull clay vault. C) The liquid polymer used to reproduce the brain was spilled in a complete skull model. After removing the vault, brain perfectly reproduced the details of gross superficial cerebral parenchyma, including: inferior frontal gyrus (IFG), middle frontal gyrus (MFG), superior frontal gyrus (SFG), precentral gyrus (Prec. G), postcentral gyrus (Postc. G.). D) The complete phantom with the vault covered with a skin-like silicon layer.

Figure 12.

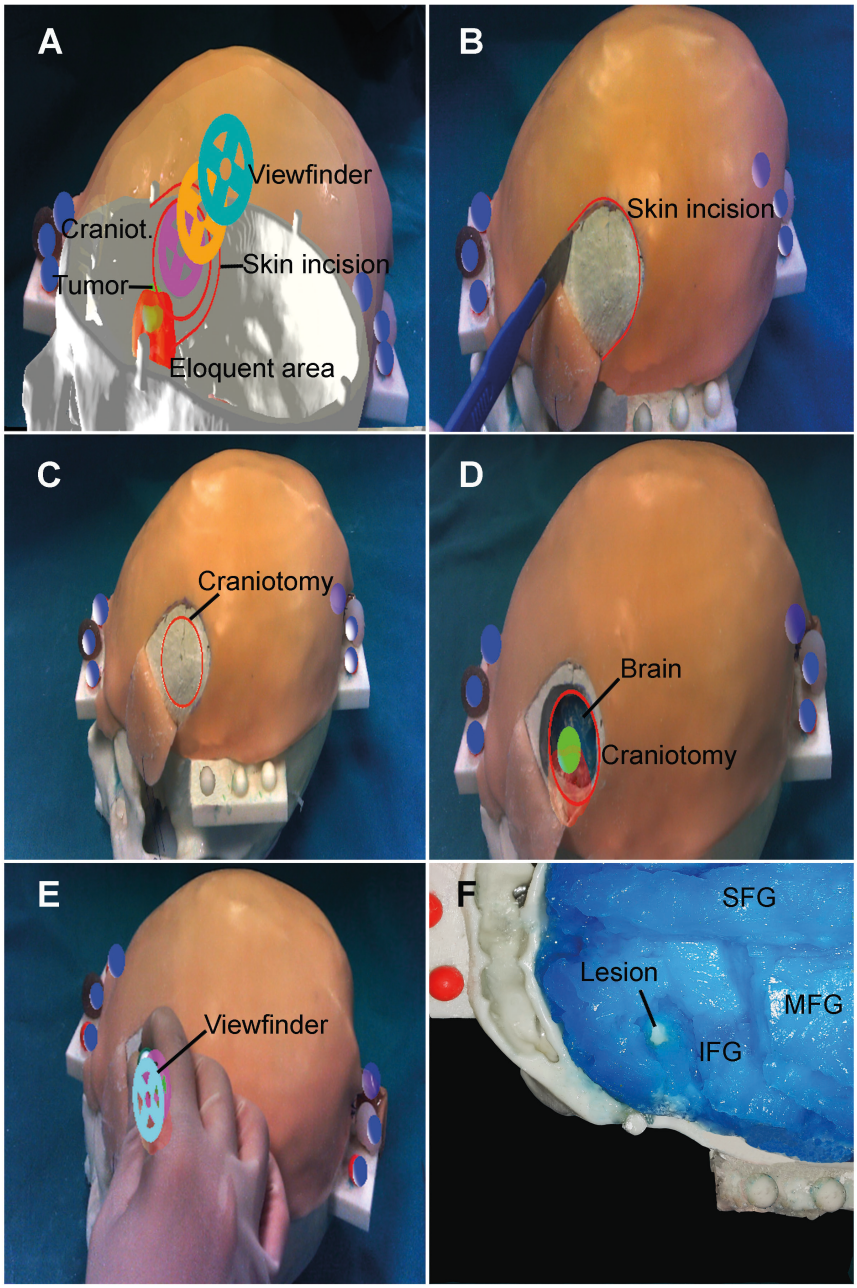

The experiment with AR. A, The complete virtual model is shown to the surgeon, including the tumor, the eloquent area (Eloq. area), three aligned viewfinders identifying the surgical trajectory, the craniotomy (Craniot.) and the skin incision. B, The skin incision is performed following the corresponding AR model. C, After removing the skin incision model, the craniotomy perimeter is displayed. D, After the craniotomy is actually performed, the lesion (green) medial to the eloquent area is shown. At this moment, by observing the superficial cortical anatomy along with the target, the surgeon can conceptualize the surgical trajectory. E, One to three pathfinders can be simultaneously shown to the neurosurgeon, in order to re-check the correct alignment of the dissecting instrument with the lesion. F. At the end of the experiment, the cranial vault is removed and the brain exposed. Since the surgical dissection passed through the inferior sulcus (namely between the inferior frontal gyrus, IFG, and the middle frontal gyrus, MFG), the anterior part of the MFG was

removed in order to demonstrate whether lesion was actually reached, and the eloquent area was avoided, as in this case. IFG, inferior frontal gyrus.

Figure 13.

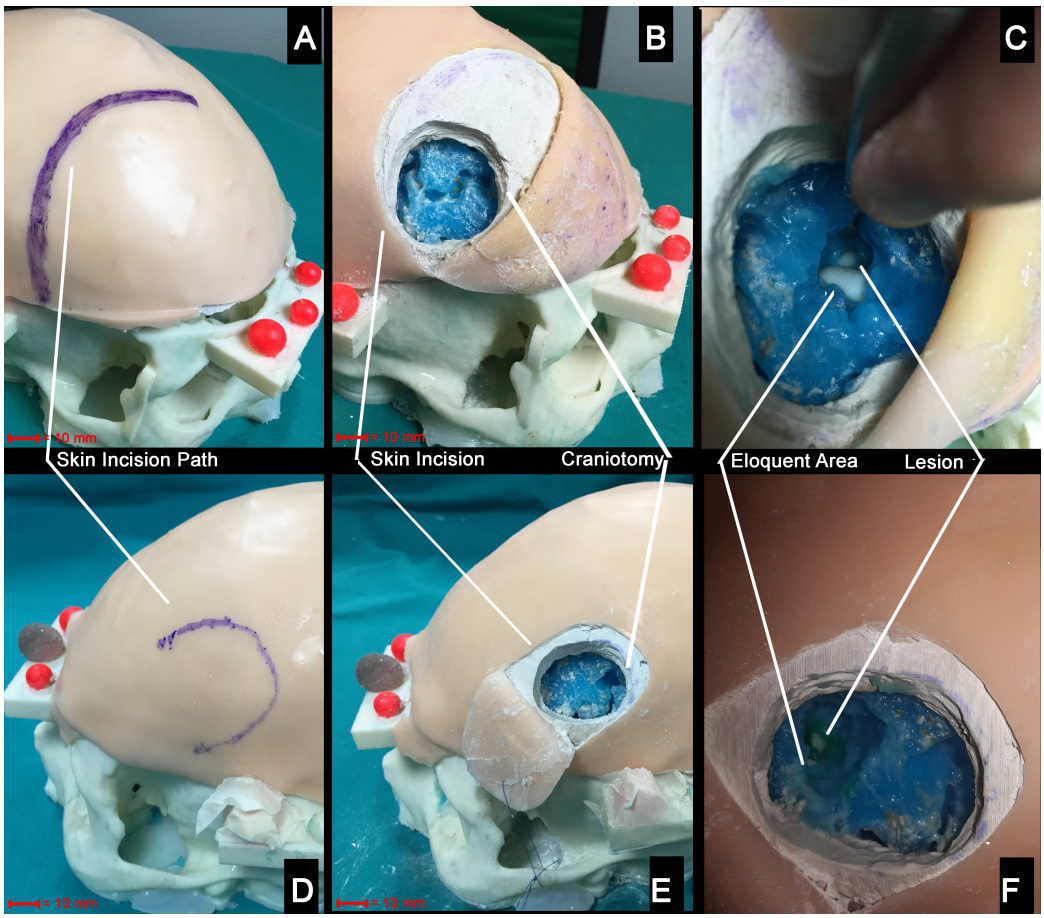

Qualitative comparison between the two approaches to accessing the lesion: augmented reality-based approach (bottom row) vs standard approach (top row).

A vs D: by using the augmented reality guidance the size of the skin incision results significantly smaller since the surgeon does not need to expose a large part of the skull vault to targeting the lesion.

B vs E: the same concept supports the fact that the osteotomy results wider with the standard approach since the surgeon needs to expose parenchyma sulci and gyri as reference landmarks to navigate towards the lesion.

C vs F: the target lesion was reached with both the approaches. However, with the standard approach (C) the eloquent area was considerably exposed (thus implying its possible damaging) and the lesion was not targeted at the center, whereas with the augmented reality approach (F) the lesion was centered and the eloquent area was only slightly exposed.

References

1. Kersten-Oertel M, Jannin P, Collins DL. DVV: a taxonomy for mixed reality visualization in image guided surgery. *IEEE Trans Vis Comput Graph.* Feb 2012;18(2):332-352.

2. Zheng G, Dong X, Gruetzner PA. Reality-augmented virtual fluoroscopy for computer-assisted diaphyseal long bone fracture osteosynthesis: a novel technique and feasibility study results. *Proc Inst Mech Eng H.* Jan 2008;222(1):101-115.

3. Bainbridge D, Jones DL, Guiraudon GM, Peters TM. Ultrasound image and augmented reality guidance for off-pump, closed, beating, intracardiac surgery. *Artif Organs.* Nov 2008;32(11):840-845.

4. Teber D, Guven S, Simpfendorfer T, et al. Augmented reality: a new tool to improve surgical accuracy during laparoscopic partial nephrectomy? Preliminary in vitro and in vivo results. *Eur Urol.* Aug 2009;56(2):332-338.

5. Soler L, Nicolau S, Pessaux P, Mutter D, Marescaux J. Real-time 3D image reconstruction guidance in liver resection surgery. *Hepatobiliary Surg Nutr.* Apr 2014;3(2):73-81.

6. Kockro RA, Tsai YT, Ng I, et al. Dex-ray: augmented reality neurosurgical navigation with a handheld video probe. *Neurosurgery.* Oct 2009;65(4):795-807; discussion 807-798.

7. Inoue D, Cho B, Mori M, et al. Preliminary study on the clinical application of augmented reality neuronavigation. *Journal of neurological surgery. Part A, Central European neurosurgery.* Mar 2013;74(2):71-76.

8. Kersten-Oertel M, Jannin P, Collins DL. The state of the art of visualization in mixed reality image guided surgery. *Comput Med Imaging Graph.* Mar 2013;37(2):98-112.

9. Jellison BJ, Field AS, Medow J, Lazar M, Salamat MS, Alexander AL. Diffusion tensor imaging of cerebral white matter: a pictorial review of physics, fiber tract anatomy, and tumor imaging patterns. *AJNR. American journal of neuroradiology.* Mar 2004;25(3):356-369.

10. Catani M, Howard RJ, Pajevic S, Jones DK. Virtual in vivo interactive dissection of white matter fasciculi in the human brain. *NeuroImage.* Sep 2002;17(1):77-94.

11. Catani M, Thiebaut de Schotten M. *Atlas of human brain connections*. Oxford ; New York: Oxford University Press; 2012.

12. Le Bihan D, Poupon C, Amadon A, Lethimonnier F. Artifacts and pitfalls in diffusion MRI. *Journal of magnetic resonance imaging : JMRI.* Sep 2006;24(3):478-488.

13. Fernandez-Miranda JC, Pathak S, Engh J, et al. High-definition fiber tractography of the human brain: neuroanatomical validation and neurosurgical applications. *Neurosurgery.* Aug 2012;71(2):430-453.

14. Van Essen DC, Smith SM, Barch DM, et al. The WU-Minn Human Connectome Project: an overview. *NeuroImage.* Oct 15 2013;80:62-79.

15. Yeh FC, Verstynen TD, Wang Y, Fernandez-Miranda JC, Tseng WY. Deterministic diffusion fiber tracking improved by quantitative anisotropy. *PloS one.* 2013;8(11):e80713.

16. Thiebaut de Schotten M, Dell'Acqua F, Forkel SJ, et al. A lateralized brain network for visuospatial attention. *Nat Neurosci.* Oct 2011;14(10):1245-1246.

17. Meola A, Comert A, Yeh FC, Stefaneanu L, Fernandez-Miranda JC. The controversial existence of the human superior fronto-occipital fasciculus: Connectome-based tractographic study with microdissection validation. *Human brain mapping.* Oct 5 2015.

18. Makris N, Papadimitriou GM, Sorg S, Kennedy DN, Caviness VS, Pandya DN. The occipitofrontal fascicle in humans: a quantitative, in vivo, DT-MRI study. *NeuroImage.* Oct 1 2007;37(4):1100-1111.

19. Wakana S, Jiang H, Nagae-Poetscher LM, van Zijl PC, Mori S. Fiber tract-based atlas of human white matter anatomy. *Radiology.* Jan 2004;230(1):77-87.

20. Ture U, Yasargil MG, Pait TG. Is there a superior occipitofrontal fasciculus? A microsurgical anatomic study. *Neurosurgery.* Jun 1997;40(6):1226-1232.

21. Kwon HG, Hong JH, Hong CP, Lee DH, Ahn SH, Jang SH. Dentatorubrothalamic tract in human brain: diffusion tensor tractography study. *Neuroradiology.* Oct 2011;53(10):787-791.

22. Lotze M, Montoya P, Erb M, et al. Activation of cortical and cerebellar motor areas during executed and imagined hand movements: an fMRI study. *Journal of cognitive neuroscience.* Sep 1999;11(5):491-501.

23. Desmond JE, Gabrieli JD, Wagner AD, Ginier BL, Glover GH. Lobular patterns of cerebellar activation in verbal working-memory and finger-tapping tasks as revealed by functional MRI. *The Journal of neuroscience : the official journal of the Society for Neuroscience.* Dec 15 1997;17(24):9675-9685.

24. Ellerman JM, Flament D, Kim SG, et al. Spatial patterns of functional activation of the cerebellum investigated using high field (4 T) MRI. *NMR in biomedicine.* Mar 1994;7(1-2):63-68.

25. Cho SS, Yoon EJ, Bang SA, et al. Metabolic changes of cerebrum by repetitive transcranial magnetic stimulation over lateral cerebellum: a study with FDG PET. *Cerebellum.* Sep 2012;11(3):739-748.

26. Miall RC, Christensen LO. The effect of rTMS over the cerebellum in normal human volunteers on peg-board movement performance. *Neuroscience letters.* Nov 23 2004;371(2-3):185-189.

27. Fisher BE, Boyd L, Winstein CJ. Contralateral cerebellar damage impairs imperative planning but not updating of aimed arm movements in humans. *Experimental brain research.* Oct 2006;174(3):453-466.

28. Immisch I, Quintern J, Straube A. Unilateral cerebellar lesions influence arm movements bilaterally. *Neuroreport.* May 6 2003;14(6):837-840.

29. Molinari M, Leggio MG, Solida A, et al. Cerebellum and procedural learning: evidence from focal cerebellar lesions. *Brain : a journal of neurology.* Oct 1997;120 (Pt 10):1753-1762.

30. Greger B, Norris SA, Thach WT. Spike firing in the lateral cerebellar cortex correlated with movement and motor parameters irrespective of the effector limb. *Journal of neurophysiology.* Jan 2004;91(1):576-582.

31. Robertson LT, Grimm RJ. Responses of primate dentate neurons to different trajectories of the limb. *Experimental brain research.* Nov 14 1975;23(5):447-462.

32. Amrani K, Dykes RW, Lamarre Y. Bilateral contributions to motor recovery in the monkey following lesions of the deep cerebellar nuclei. *Brain research.* Nov 18 1996;740(1-2):275-284.

33. Beaubaton D, Trouche E. Participation of the cerebellar dentate nucleus in the control of a goal-directed movement in monkeys. Effects of reversible or permanent dentate lesion on the duration and accuracy of a pointing response. *Experimental brain research.* 1982;46(1):127-138.

34. Meola A, Comert A, Yeh FC, Sivakanthan S, Fernandez-Miranda JC. The nondecussating pathway of the dentatorubrothalamic tract in humans: human connectome-based tractographic study and microdissection validation. *Journal of neurosurgery.* Oct 9 2015:1-7.

35. Meola A, Fernandez-Miranda JC. Peduncles Without Cerebellum: The Cerebellar Agenesis. *Eur Neurol.* Oct 10 2015;74(3-4):162.

36. Ford AA, Colon-Perez L, Triplett WT, Gullett JM, Mareci TH, Fitzgerald DB. Imaging white matter in human brainstem. *Frontiers in human neuroscience.* 2013;7:400.

37. Habas C, Cabanis EA. Anatomical parcellation of the brainstem and cerebellar white matter: a preliminary probabilistic tractography study at 3 T. *Neuroradiology.* Oct 2007;49(10):849-863.

38. Kamali A, Kramer LA, Butler IJ, Hasan KM. Diffusion tensor tractography of the somatosensory system in the human brainstem: initial findings using high isotropic spatial resolution at 3.0 T. *European radiology.* Jun 2009;19(6):1480-1488.

39. Mamata H, Mamata Y, Westin CF, et al. High-resolution line scan diffusion tensor MR imaging of white matter fiber tract anatomy. *AJNR. American journal of neuroradiology.* Jan 2002;23(1):67-75.

40. Nagae-Poetscher LM, Jiang H, Wakana S, Golay X, van Zijl PC, Mori S. High-resolution diffusion tensor imaging of the brain stem at 3 T. *AJNR. American journal of neuroradiology.* Sep 2004;25(8):1325-1330.

41. Prats-Galino A, Soria G, de Notaris M, Puig J, Pedraza S. Functional anatomy of subcortical circuits issuing from or integrating at the human brainstem. *Clinical neurophysiology : official journal of the International Federation of Clinical Neurophysiology.* Jan 2012;123(1):4-12.

42. Salamon N, Sicotte N, Alger J, et al. Analysis of the brain-stem white-matter tracts with diffusion tensor imaging. *Neuroradiology.* Dec 2005;47(12):895-902.

43. Stieltjes B, Kaufmann WE, van Zijl PC, et al. Diffusion tensor imaging and axonal tracking in the human brainstem. *NeuroImage.* Sep 2001;14(3):723-735.

44. Rowley HA, Roberts TP. Functional localization by magnetoencephalography. *Neuroimaging clinics of North America.* Nov 1995;5(4):695-710.

45. Gallen CC, Schwartz BJ, Bucholz RD, et al. Presurgical localization of functional cortex using magnetic source imaging. *Journal of neurosurgery.* Jun 1995;82(6):988-994.

46. Kamada K, Takeuchi F, Kuriki S, Oshiro O, Houkin K, Abe H. Functional neurosurgical simulation with brain surface magnetic resonance images and magnetoencephalography. *Neurosurgery.* Aug 1993;33(2):269-272; discussion 272-263.

47. Lutkenhoner B, Krumbholz K, Lammertmann C, Seither-Preisler A, Steinstrater O, Patterson RD. Localization of primary auditory cortex in humans by magnetoencephalography. *NeuroImage.* Jan 2003;18(1):58-66.

48. Plomp G, Leeuwen C, Ioannides AA. Functional specialization and dynamic resource allocation in visual cortex. *Human brain mapping.* Jan 2010;31(1):1-13.

49. Picht T, Schmidt S, Brandt S, et al. Preoperative functional mapping for rolandic brain tumor surgery: comparison of navigated transcranial magnetic stimulation to direct cortical stimulation. *Neurosurgery.* Sep 2011;69(3):581-588; discussion 588.

50. Duffau H. *Brain mapping : from neural basis of cognition to surgical applications*. Wien ; New York: Springer; 2011.

51. Logothetis NK. What we can do and what we cannot do with fMRI. *Nature.* Jun 12 2008;453(7197):869-878.

52. Milgram P, Kishino F. A Taxonomy of Mixed Reality Visual-Displays. *Ieice T Inf Syst.* Dec 1994;E77d(12):1321-1329.

53. Badiali G, Ferrari V, Cutolo F, et al. Augmented reality as an aid in maxillofacial surgery: Validation of a wearable system allowing maxillary repositioning. *Journal of Cranio-Maxillofacial Surgery.* 2014(0).

54. Rhoton AL, Rhoton AL, Congress of Neurological Surgeons. *Rhoton cranial anatomy and surgical approaches*. Philadelphia: Lippincott Williams & Wilkins; 2003.

55. Perneczky A, Reisch R, Tschabitscher M. *Keyhole approaches in neurosurgery*. Wien ; New York: Springer; 2008.

56. Kersten-Oertel M, Jannin P, Collins DL. DVV: Towards a Taxonomy for Mixed Reality Visualization in Image Guided Surgery. *Lect Notes Comput Sc.* 2010;6326:334-343.

57. Kawamata T, Iseki H, Shibasaki T, Hori T. Endoscopic augmented reality navigation system for endonasal transsphenoidal surgery to treat pituitary tumors: technical note. *Neurosurgery.* Jun 2002;50(6):1393-1397.

58. King AP, Edwards PJ, Maurer CR, Jr., et al. A system for microscope-assisted guided interventions. *Stereotact Funct Neurosurg.* 1999;72(2-4):107-111.

59. Edwards PJ, Johnson LG, Hawkes DJ, Fenlon MR, Strong A, Gleeson M. Clinical experience and perception in stereo augmented reality surgical navigation. In: Z. YG, Jiang T, eds. *MIAR*. Berlin Heidelberg Springer-Verlag; 2004:369-376.

60. Lovo EE, Quintana JC, Puebla MC, et al. A novel, inexpensive method of image coregistration for applications in image-guided surgery using augmented reality. *Neurosurgery.* Apr 2007;60(4 Suppl 2):366-371; discussion 371-362.

61. Masutani Y, Dohi T, Yamane F, Iseki H, Takakura K. Augmented reality visualization system for intravascular neurosurgery. *Comput Aided Surg.* 1998;3(5):239-247.

62. Cabrilo I, Bijlenga P, Schaller K. Augmented reality in the surgery of cerebral arteriovenous malformations: technique assessment and considerations. *Acta neurochirurgica.* Sep 2014;156(9):1769-1774.

63. Cabrilo I, Bijlenga P, Schaller K. Augmented reality in the surgery of cerebral aneurysms: a technical report. *Neurosurgery.* Jun 2014;10 Suppl 2:252-260; discussion 260-251.

64. Iseki H, Masutani Y, Iwahara M, et al. Volumegraph (overlaid three-dimensional image-guided navigation). Clinical application of augmented reality in neurosurgery. *Stereotact Funct Neurosurg.* 1997;68(1-4 Pt 1):18-24.

65. Deng W, Li F, Wang M, Song Z. Easy-to-use augmented reality neuronavigation using a wireless tablet PC. *Stereotact Funct Neurosurg.* 2014;92(1):17-24.

66. Cabrilo I, Schaller K, Bijlenga P. Augmented reality-assisted bypass surgery: embracing minimal invasiveness. *World neurosurgery.* Apr 2015;83(4):596-602.

67. Liberati A, Altman DG, Tetzlaff J, et al. The PRISMA statement for reporting systematic reviews and meta-analyses of studies that evaluate healthcare interventions: explanation and elaboration. *BMJ.* 2009;339:b2700.

68. Doyle WK. Low end interactive image-directed neurosurgery. Update on rudimentary augmented reality used in epilepsy surgery. *Stud Health Technol Inform.* 1996;29:1-11.

69. Stadie AT, Reisch R, Kockro RA, et al. Minimally invasive cerebral cavernoma surgery using keyhole approaches - solutions for technique-related limitations. *Minimally invasive neurosurgery : MIN.* Feb 2009;52(1):9-16.

70. Kantelhardt SR, Gutenberg A, Neulen A, Keric N, Renovanz M, Giese A. Video-Assisted Navigation for Adjustment of Image-Guidance Accuracy to Slight Brain Shift. *Neurosurgery.* Jul 30 2015.

71. Paul P, Fleig O, Jannin P. Augmented virtuality based on stereoscopic reconstruction in multimodal image-guided neurosurgery: methods and performance evaluation. *IEEE Trans Med Imaging.* Nov 2005;24(11):1500-1511.

72. Ferrari V, Megali G, Troia E, Pietrabissa A, Mosca F. A 3-D mixed-reality system for stereoscopic visualization of medical dataset. *IEEE Trans Biomed Eng.* Nov 2009;56(11):2627-2633.

73. Drouin S, Kersten-Oertel M, Collins DL. Interaction-Based Registration Correction for Improved Augmented Reality Overlay in Neurosurgery. In: Linte C, Yaniv Z, Fallavollita P, eds. *Augmented Environments for Computer-Assisted Interventions.* Vol 9365: Springer International Publishing; 2015:21-29.

74. Low D, Lee CK, Dip LL, Ng WH, Ang BT, Ng I. Augmented reality neurosurgical planning and navigation for surgical excision of parasagittal, falcine and convexity meningiomas. *Br J Neurosurg.* Feb 2010;24(1):69-74.

75. Besharati Tabrizi L, Mahvash M. Augmented reality-guided neurosurgery: accuracy and intraoperative application of an image projection technique. *Journal of neurosurgery.* Jul 2015;123(1):206-211.

76. Wang J, Suenaga H, Hoshi K, et al. Augmented reality navigation with automatic marker-free image registration using 3-d image overlay for dental surgery. *IEEE Trans Biomed Eng.* Apr 2014;61(4):1295-1304.

77. Zhang X, Chen G, Liao H. A High-accuracy Surgical Augmented Reality System Using Enhanced Integral Videography Image Overlay. Paper presented at: 37th Annual International Conference of the IEEE Engineering in Medicine and Biology Society EMBC2015; Milano.

78. Levoy M. Light fields and computational imaging. *Computer.* 2006(8):46-55.

79. Lippmann G. Epreuves reversibles donnant la sensation du relief. *J. Phys. Theor. Appl.* 1908;7(1):821-825.

80. Cutolo F, Badiali G, Ferrari V. Human-PnP: Ergonomic AR Interaction Paradigm for Manual Placement of Rigid Bodies. *Augmented Environments for Computer-Assisted Interventions*: Springer International Publishing; 2015:50-60.

81. Craig AB. *Understanding augmented reality : concepts and applications*. Waltham, MA: Morgan Kaufmann; 2013.

82. Le Moigne J, Netanyahu NS, Eastman RD. *Image registration for remote sensing*. Cambridge ; New York: Cambridge University Press; 2010.

83. Kruijff E, Swan JE, Feiner S. Perceptual issues in augmented reality revisited. Paper presented at: Mixed and Augmented Reality (ISMAR), 2010 9th IEEE International Symposium on; 13-16 Oct. 2010, 2010.

84. Reichelt S, Häussler R, Fütterer G, Leister N. Depth cues in human visual perception and their realization in 3D displays. Paper presented at: SPIE Defense, Security, and Sensing2010.

85. Kersten-Oertel M, Chen SJ, Collins DL. An evaluation of depth enhancing perceptual cues for vascular volume visualization in neurosurgery. *IEEE Trans Vis Comput Graph.* Mar 2014;20(3):391-403.

86. Cutolo F, Parchi PD, Ferrari V. Video See Through AR Head-Mounted Display for Medical Procedures. *Int Sym Mix Augment.* 2014:393-396.

87. Ferrari V, Cutolo F, Calabro EM, Ferrari M. HMD Video See Though AR with Unfixed Cameras Vergence. *Int Sym Mix Augment.* 2014:265-266.

88. Ferrari V, Megali G, Troia E, Pietrabissa A, Mosca F. A 3-D Mixed-Reality System for Stereoscopic Visualization of Medical Dataset. *Ieee T Bio-Med Eng.* Nov 2009;56(11):2627-2633.

89. Zhang ZY. A flexible new technique for camera calibration. *Ieee T Pattern Anal.* Nov 2000;22(11):1330-1334.

90. Cutolo F, Badiali G, Ferrari V. Human-PnP: Ergonomic AR Interaction Paradigm for Manual Placement of Rigid Bodies. In: Linte C, Yaniv Z, Fallavollita P, eds. *Augmented Environments for Computer-Assisted Interventions.* Vol 9365: Springer International Publishing; 2015:50-60.

91. Navab N, Heining SM, Traub J. Camera Augmented Mobile C-Arm (CAMC): Calibration, Accuracy Study, and Clinical Applications. *Ieee T Med Imaging.* Jul 2010;29(7):1412-1423.

92. Ferrari V, Carbone M, Cappelli C, et al. Value of multidetector computed tomography image segmentation for preoperative planning in general surgery. *Surgical Endoscopy and Other Interventional Techniques.* Mar 2012;26(3):616-626.

93. Condino S, Carbone M, Ferrari V, et al. How to build patient-specific synthetic abdominal anatomies. An innovative approach from physical toward hybrid surgical simulators. *The international journal of medical robotics + computer assisted surgery : MRCAS.* Jun 2011;7(2):202-213.

94. Chen SJ, Hellier P, Marchal M, et al. An anthropomorphic polyvinyl alcohol brain phantom based on Colin27 for use in multimodal imaging. *Medical physics.* Jan 2012;39(1):554-561.

95. Chiarelli P, Lanata A, Carbone M. Acoustic waves in hydrogels: A bi-phasic model for ultrasound tissue-mimicking phantom. *Mat Sci Eng C-Bio S.* Apr 30 2009;29(3):899-907.

96. Pietrabissa A, Morelli L, Ferrari M, et al. Mixed reality for robotic treatment of a splenic artery aneurysm. *Surg Endosc.* May 2010;24(5):1204.

97. Parrini S, Cutolo F, Freschi C, Ferrari M, Ferrari V. Augmented reality system for freehand guide of magnetic endovascular devices. *Conf Proc IEEE Eng Med Biol Soc.* Aug 2014;2014:490-493.

98. Badiali G, Ferrari V, Cutolo F, et al. Augmented reality as an aid in maxillofacial surgery: validation of a wearable system allowing maxillary repositioning. *J Craniomaxillofac Surg.* Dec 2014;42(8):1970-1976.

99. Mahvash M, Besharati Tabrizi L. A novel augmented reality system of image projection for image-guided neurosurgery. *Acta neurochirurgica.* May 2013;155(5):943-947.

100. Edwards PJ, King AP, Maurer CR, Jr., et al. Design and evaluation of a system for microscope-assisted guided interventions (MAGI). *IEEE Trans Med Imaging.* Nov 2000;19(11):1082-1093.

.